THE JOURNAL OF BIOLOGICAL CHEMISTRY VOL. 289, NO. 49, pp. 33887–33903, December 5, 2014

Arf6 Guanine Nucleotide Exchange Factor Cytohesin-2 Binds to CCDC120 and Is Transported Along Neurites to Mediate Neurite Growth*[S]

Received for publication, April 24, 2014, and in revised form, October 7, 2014 Published, JBC Papers in Press, October 17, 2014, DOI 10.1074/jbc.M114.575787

Tomohiro Torii[‡1,2], **Yuki Miyamoto**[‡], **Kenji Tago**[§], **Kazunori Sango**[¶], **Kazuaki Nakamura**[‡], **Atsushi Sanbe**[‖], **Akito Tanoue**[‡1], **and Junji Yamauchi**[‡**3]

*From the [‡]Department of Pharmacology, National Research Institute for Child Health and Development, Setagaya, Tokyo 157-8535, the [§]Graduate School of Medicine, Jichi Medical University, Shimotsuke, Tochigi 329-0498, the [¶]Amyotrophic Lateral Sclerosis/Neuropathy Project, Tokyo Metropolitan Institute of Medical Science, Setagaya, Tokyo 156-8506, the [‖]School of Pharmacy, Iwate Medical University, Morioka, Iwate 020-0023, and the **Graduate School of Medical and Dental Sciences, Tokyo Medical and Dental University, Bunkyo, Tokyo 113-8510, Japan*

Background: The Arf6 activator, cytohesin-2, is involved in neurite growth.
Results: Cytohesin-2 binds to CCDC120 and is transported along growing neurites.
Conclusion: This interaction is required for Arf6 activation and neurite growth.
Significance: The previously unknown functional CCDC120 is a new cytohesin adaptor protein, which regulates neurite growth.

The mechanism of neurite growth is complicated, involving continuous cytoskeletal rearrangement and vesicular trafficking. Cytohesin-2 is a guanine nucleotide exchange factor for Arf6, an Arf family molecular switch protein, controlling cell morphological changes such as neuritogenesis. Here, we show that cytohesin-2 binds to a protein with a previously unknown function, CCDC120, which contains three coiled-coil domains, and is transported along neurites in differentiating N1E-115 cells. Transfection of the small interfering RNA (siRNA) specific for CCDC120 into cells inhibits neurite growth and Arf6 activation. When neurites start to extend, vesicles containing CCDC120 and cytohesin-2 are transported in an anterograde manner rather than a retrograde one. As neurites continue extension, anterograde vesicle transport decreases. CCDC120 knockdown inhibits cytohesin-2 localization into vesicles containing CCDC120 and diffuses cytohesin-2 in cytoplasmic regions, illustrating that CCDC120 determines cytohesin-2 localization in growing neurites. Reintroduction of the wild type CCDC120 construct into cells transfected with CCDC120 siRNA reverses blunted neurite growth and Arf6 activity, whereas the cytohesin-2-binding CC1 region-deficient CCDC120 construct does not. Thus, cytohesin-2 is transported along neurites by vesicles containing CCDC120, and it mediates neurite growth. These results suggest a mechanism by which guanine nucleotide exchange factor for Arf6 is transported to mediate neurite growth.

In the developing nervous system, neuronal cells continuously change their morphology and undergo neurite outgrowth, axon navigation, and synaptogenesis to form neural networks (1). Neurite outgrowth is a complicated process and involves various dynamic molecular mechanisms (2–5). For example, membrane, cytoskeletal, and signaling components are continuously transported along growing neurites (6, 7).

Arfs belong to the small guanine nucleotide-binding protein family. Similar to Ras and Rho GTPases, Arfs also act as molecular switches; they are biologically active when bound to GTP and are inactive when bound to GDP. Mammalian Arfs are grouped into three classes as follows: class I (Arf1 and Arf2 and/or Arf3), class II (Arf4 and Arf5), and class III (Arf6) (8–11). Among them, Arf6 is a unique Arf protein because its primary role is to control cytoskeletal rearrangement, whereas that of the other Arfs is to regulate intracellular membrane trafficking (8, 9). Two types of proteins, guanine nucleotide exchange factors (GEFs)[4] and GTPase-activating proteins, strictly control the Arf6 guanine nucleotide-binding state. The former reaction is important because GEFs define the strength and/or the cellular compartment to activate Arf6 by integrating the upstream signals (10, 11). Cytohesin-2 is such a protein and is one of four cytohesins (12, 13). All cytohesins are composed of the same domain structure as follows: the N-terminal coiled-coil (CC) domain, the catalytic Sec7 domain, the phospho-

* This work has been supported by grants-in-aid for young scientists, Scientific Research B, and Scientific Research on Innovative Areas, "Glial Assembly: A New Regulatory Machinery of Brain Function and Disorders" from the Japanese Ministry of Education, Culture, Sports, Science, and Technology and the Japanese Ministry of Health, Labour, and Welfare, and in part by grants from the Takeda Science Foundation and the Uehara Science Foundation.
[S] This article contains supplemental Movies 1–4.
[1] Both authors contributed equally to this work.
[2] To whom correspondence may be addressed: Dept. of Pharmacology, National Research Institute for Child Health and Development, 2-10-1 Okura, Setagaya, Tokyo 157-8535, Japan. Tel.: 81-3-5494-7120 (Ext. 4670); Fax: 81-3-5494-7057; E-mail: torii-t@ncchd.go.jp.
[3] To whom correspondence may be addressed: Dept. of Pharmacology, National Research Institute for Child Health and Development, 2-10-1 Okura, Setagaya, Tokyo 157-8535, Japan. Tel.: 81-3-5494-7120 (Ext. 4670); Fax: 81-3-5494-7057; E-mail: yamauchi-j@ncchd.go.jp.

[4] The abbreviations used are: GEF, guanine nucleotide exchange factor; CC, coiled-coil; RFP, red fluorescent protein; PH, pleckstrin homology; ANOVA, analysis of variance; EGFP, enhanced GFP.

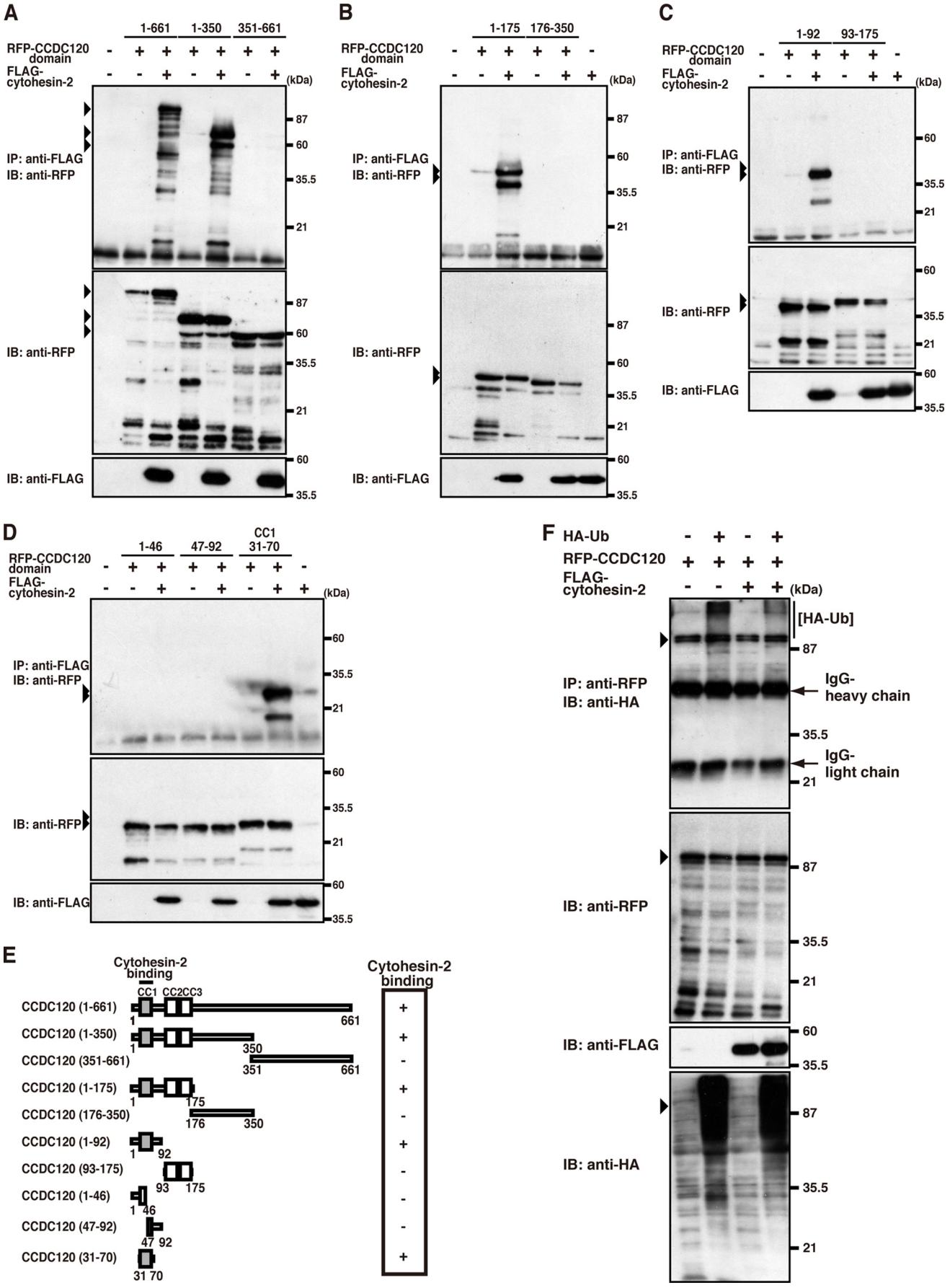
A
1-661
1-350
351-661
RFP-CCDC120 domain
FLAG-cytohesin-2
(kDa)
IP: anti-FLAG
IB: anti-RFP
IB: anti-RFP
IB: anti-FLAG
B
1-175
176-350
RFP-CCDC120 domain
FLAG-cytohesin-2
(kDa)
IP: anti-FLAG
IB: anti-RFP
IB: anti-RFP
IB: anti-FLAG
C
1-92
93-175
RFP-CCDC120 domain
FLAG-cytohesin-2
(kDa)
IP: anti-FLAG
IB: anti-RFP
IB: anti-RFP
IB: anti-FLAG
D
1-46
47-92
CC1 31-70
RFP-CCDC120 domain
FLAG-cytohesin-2
(kDa)
IP: anti-FLAG
IB: anti-RFP
IB: anti-RFP
IB: anti-FLAG
E
Cytohesin-2 binding
CC1
CC2
CC3
CCDC120 (1-661)
CCDC120 (1-350)
CCDC120 (351-661)
CCDC120 (1-175)
CCDC120 (176-350)
CCDC120 (1-92)
CCDC120 (93-175)
CCDC120 (1-46)
CCDC120 (47-92)
CCDC120 (31-70)
Cytohesin-2 binding
F
HA-Ub
RFP-CCDC120
FLAG-cytohesin-2
(kDa)
[HA-Ub]
IP: anti-RFP
IB: anti-HA
IgG-heavy chain
IgG-light chain
IB: anti-RFP
IB: anti-FLAG
IB: anti-HA

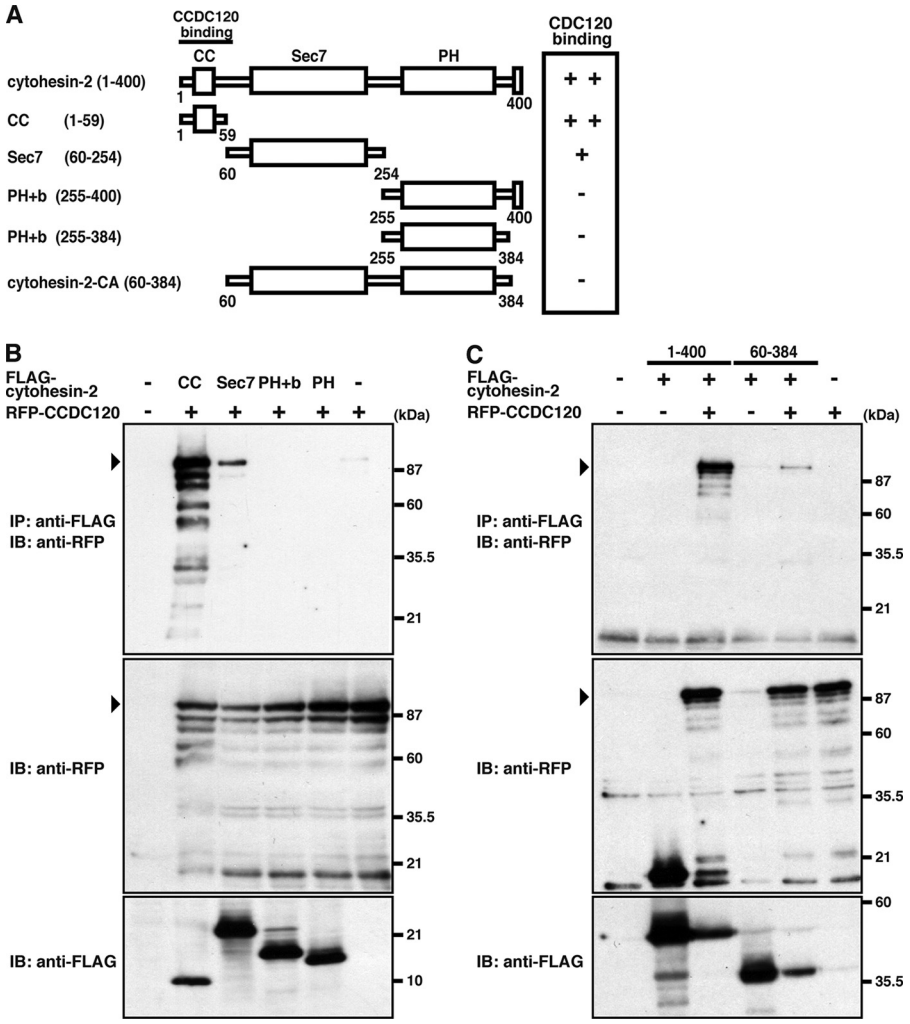

FIGURE 2. **Interaction of cytohesin-2 and CCDC120 are mediated by the CC domain of cytohesin-2 in mammalian cells.** *A,* schematic structures of full-length (wild type) cytohesin-2 and the domains are illustrated (number shows amino acid's one). *B* and *C,* 293T cells were transfected with plasmids coding either FLAG-tagged CCDC120 domain (full-length(1–400), CC(1–59), Sec7(60–254), PH+b(255–400), PH(255–384), and cytohesin-2-CA(60–384 amino acids)) or RFP-CCDC120. Cytohesin-2-CA is characterized as a constitutively active form of cytohesin-2 in previous study (14). After 48 h, cells were lysed. Cell lysates were immunoprecipitated (*IP*) with an anti-FLAG antibody and immunoblotted (*IB*) with an anti-RFP antibody. The total lysates were also used for immunoblotting with an anti-RFP antibody or anti-FLAG antibody. *Arrowheads* indicate the position of RFP fusion proteins.

inositide-binding pleckstrin homology (PH) domain, and the C-terminal polybasic amino acid region (14).

We previously reported that cytohesin-2 and downstream Arf6 activation participate in promoting neurite extension (15) and that cytohesin-2 regulates its extension through the cytoskeletal protein actinin at the growth cone in mouse neuroblastoma N1E-115 cells (16). However, the mechanism of Arf6-GEF cytohesin-2 transport along growing neurites has not been resolved. In this study, we demonstrate that a protein, CC domain-containing protein 120 (CCDC120), which had a previously unknown function, is the binding partner that determines cytohesin-2 localization and mediates Arf6 activation and neurite growth. Cytohesin-2 is transported along growing neurites in vesicles containing CCDC120. These results present

FIGURE 1. **CCDC120 binds to cytohesin-2 through the CC1 domain.** *A,* 293T cells were transfected with plasmids coding either RFP-tagged CCDC120 region (1–661, 1–350, and 351–661 amino acids) or FLAG-cytohesin-2. After 48 h, cells were lysed. Cell lysates were immunoprecipitated (*IP*) with an anti-FLAG antibody and immunoblotted with an anti-RFP antibody. The total lysates were also used for immunoblotting (*IB*) with an anti-RFP antibody or anti-FLAG antibody. *Arrowheads* indicate the position of RFP fusion proteins. *B,* 293T cells were transfected with plasmids coding either RFP-tagged CCDC120 region (1–175 and 176–350 amino acids) or FLAG-cytohesin-2. After 48 h, cells were lysed. Cell lysates were immunoprecipitated with an anti-FLAG antibody and immunoblotted with an anti-RFP antibody. The total lysates were also used for immunoblotting with an anti-RFP antibody or anti-FLAG antibody. *Arrowheads* indicate the position of RFP fusion proteins. *C,* 293T cells were transfected with plasmids coding either RFP-tagged CCDC120 region (1–92 and 93–175 amino acids) or FLAG-cytohesin-2. After 48 h, cells were lysed. Cell lysates were immunoprecipitated with an anti-FLAG antibody and immunoblotted with an anti-RFP antibody. The total lysates were also used for immunoblotting with an anti-RFP antibody or anti-FLAG antibody. *Arrowheads* indicate the position of RFP fusion proteins. *D,* 293T cells were transfected with the plasmids coding for FLAG-tagged cytohesin-2 with or without either of the RFP-tagged CCDC120 domains. After 48 h, cells were lysed. The immunoprecipitates with an anti-FLAG antibody were immunoblotted with an anti-RFP antibody. Total expressed proteins are also shown. *Arrowheads* indicate the position of RFP-CCDC120 domains. *E,* schematic structures of wild type full-length CCDC120 and their domains (*numbers* indicate domains of the amino acid). *F,* 293T cells were transfected with plasmids coding either RFP-tagged full-length CCDC120, FLAG-tagged cytohesin-2, or HA-tagged ubiquitin. After 48 h, cells were lysed. Cell lysates were immunoprecipitated with an anti-RFP antibody and immunoblotted with an anti-HA antibody. The total lysates were also used for immunoblotting with an anti-RFP antibody, anti-HA antibody, or anti-FLAG antibody. *Arrowheads* indicate the position of RFP-fusion full-length CCDC120.

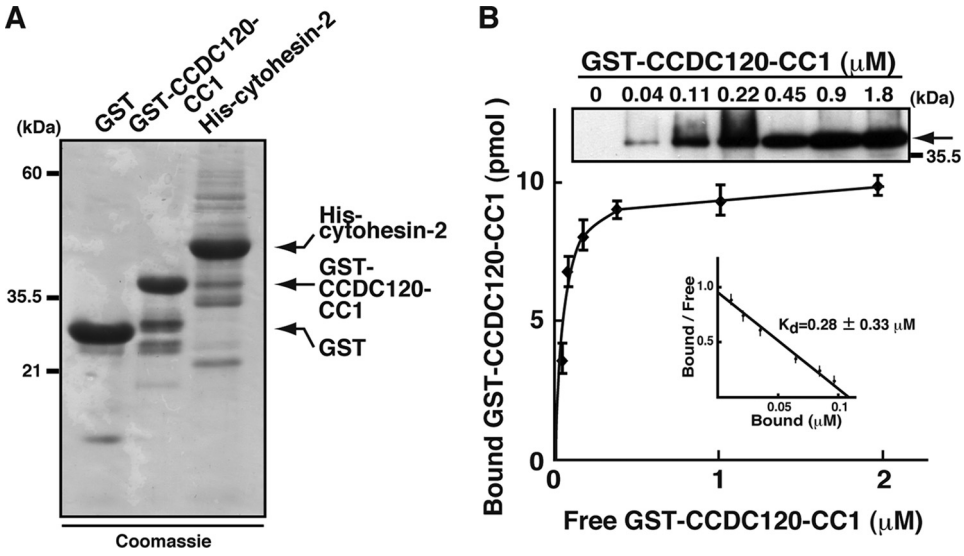

FIGURE 3. **Direct binding of GST-CCDC120-CC1 to cytohesin-2.** *A,* recombinant GST, GST-CCDC120-CC1, and His-cytohesin-2 were purified from *E. coli* and stained with Coomassie Brilliant Blue. *Arrows* indicate GST, GST-CCDC120-CC1, or His-cytohesin-2. *B,* quantitative analysis of the interaction between GST-CCDC120-CC1 and His-cytohesin-2 was performed. Various concentrations (0.04 to 1.8 μM) of recombinant GST-CCDC120-CC1 were added to an immobilized His-cytohesin-2 (0.5 μg) in 500 μl of buffer. Bound GST-CCDC120-CC1 (indicated by an *arrow*) was detected by immunoblotting with an anti-GST antibody. Amounts of the free and bound GST fusion protein were calculated by determining the protein amounts from the supernatant and pellet fractions. The amount of bound *versus* free GST-CCDC120-CC1 was plotted in a line graph (see *inset*). Scatchard analysis indicates that the K_d value was 0.28 ± 0.033 μM. Results are means ± S.D. for three independent experiments.

evidence of how a GEF for Arf6 is transported to mediate Arf6 activation and neurite growth.

EXPERIMENTAL PROCEDURES

Antibodies—Rabbit polyclonal CCDC120 antibody was purchased from ProteinTech (Chicago, IL; 1:500 for immunoblotting and immunofluorescence). Rabbit serum for cytohesin-2 was generated against a CRKKRISVKKKQEQ peptide, which was synthesized by IWAKI (Tokyo, Japan). The polyclonal anti-cytohesin-2 antibody was affinity-purified using an antigen peptide-conjugated resin and used for immunoblotting (1:500). The mouse monoclonal cytohesin-2 was purchased from Santa Cruz Biotechnology (1:50 for immunofluorescence). The mouse monoclonal active Arf6 was purchased from NewEast BioScience (Malvern, PA; 1:100 for immunofluorescence). The following antibodies (dilution used for immunoblotting) were purchased: mouse monoclonal anti-Arf6 (1:50; Santa Cruz Biotechnology); mouse monoclonal and rabbit polyclonal anti-GFP (1:1,000; MBL, Nagoya, Japan); rabbit polyclonal anti-RFP (1:1,000; Evrogen, Moscow, Russia); mouse monoclonal anti-FLAG (1:1,000; Sigma); mouse monoclonal anti-β-actin (1:1,000; BD Biosciences); horseradish peroxidase-labeled secondary antibodies (1:10,000; GE Healthcare); and fluorescence-labeled secondary antibodies (1:500; Invitrogen).

Plasmids for Mammalian Cell Expression—The pRK5-HA-ubiquitin plasmid was purchased from Addgene (Cambridge, MA). The p3×FLAG-cytohesin-2 and the plasmids encoding the domain were constructed as described in our previous reports (16–18). Human CCDC120 cDNA was obtained from the Biological Resource Center of the National Institute of Technology and Evaluation (Chiba, Japan). The domains (amino acids 1–350, 351–661, 1–175, 176–350, 1–92, 93–175, 1–46, 47–92, and amino acids 31–70) were constructed using PCR and inserted into pTagRFP-C vector (Evrogen). The CCDC120-ΔCC1 mutant (deleted amino acids 31–70) was also produced using PCR and subcloned into pTagRFP-C. Rab8b, Rab11, VAMP2, VAMP4, and VAMP7 were amplified in N1E-115 cell cDNA by the PCR method and subcloned into pEGFP-C1 vectors. All nucleotide sequences were confirmed by the Fasmac sequencing service (Kanagawa, Japan).

Recombinant Proteins—Recombinant GST and GST-GGA3 (16, 17) were produced using *Escherichia coli* BL21(DE3)pLysS (TaKaRa Bio, Kyoto, Japan) and purified according to the manufacturer's protocol for a glutathione-Sepharose 4B (GE Healthcare). Recombinant GST-CCDC120-CC1 (amino acids 31–70) was also purified using *E. coli* BL21(DE3)pLysS. The pET42a vector-based transformed *E. coli* was treated with 0.4 mM isopropyl 1-thio-β-D-galactopyranoside at 30 °C for 2.5 h and harvested by centrifugation. The precipitates were extracted with buffer A (50 mM Tris-HCl (pH 7.5), 5 mM $MgCl_2$, 1 mM dithiothreitol, 1 mM phenylmethanesulfonyl fluoride, 1 mg/ml leupeptin, 1 mM EDTA, and 0.5% Nonidet P-40) containing 500 μg/ml lysozyme and 100 μg/ml DNase I on ice. All purification steps were performed at 4 °C. The centrifuged supernatants were applied to a glutathione-Sepharose 4B column (GE Healthcare). The resins were washed with buffer B (100 mM Tris-HCl (pH 8.0), 2 mM $MgCl_2$, 1 mM dithiothreitol, 1 mM phenylmethanesulfonyl fluoride, and 1 μg/ml leupeptin). Recombinant proteins were eluted with buffer B containing 20 mM glutathione. The eluted fractions were dialyzed against buffer C (10 mM HEPES-NaOH (pH 7.5), 1 mM dithiothreitol, 2 mM $MgCl_2$, 1 mM dithiothreitol, 1 mM phenylmethanesulfonyl fluoride, 1 μg/ml leupeptin, and 150 mM NaCl) and stored at −80 °C until use. Recombinant His-tagged cytohesin-2 was produced using *E. coli* BL21(DE3)pLysS and purified according to the manufacturer's protocol for a nickel-nitrilotriacetic acid resin (GE Healthcare). In brief, *E. coli* was lysed in

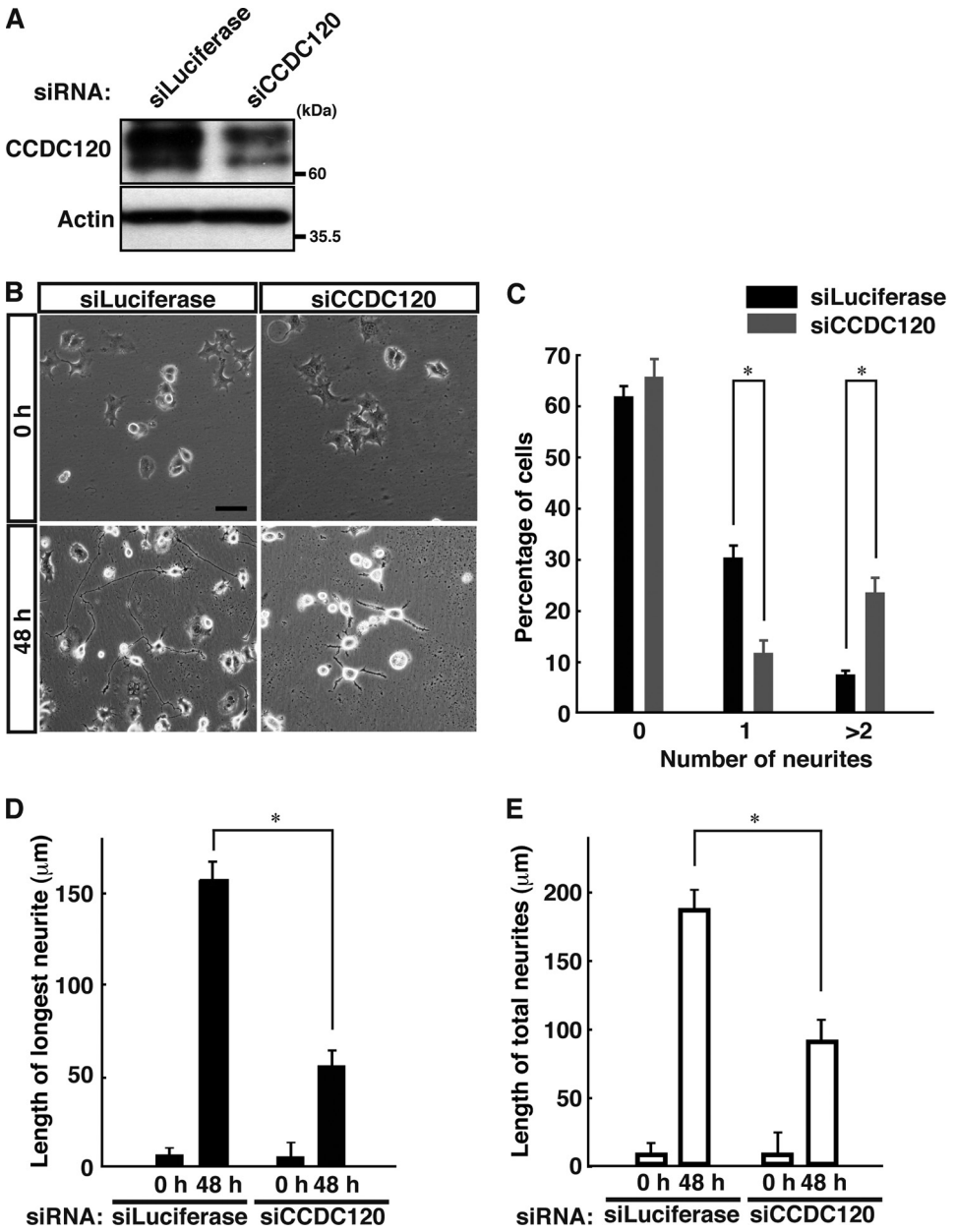

FIGURE 4. **CCDC120 is involved in neurite growth in N1E-115 cells.** *A,* N1E-115 cells were transfected with an siRNA for control luciferase or CCDC120. The expression levels of CCDC120 and actin were examined with immunoblotting using the respective antibodies. *B* and *C,* N1E-115 cells were transfected with an siRNA for control luciferase or CCDC120. Representative images are also shown at 48 h following induction of differentiation. Cells with processes longer than two cell bodies were counted as cells bearing neurites. Knockdown of CCDC120 decreased the numbers of cells with a single neurite and increased the numbers of cells with multiple neurites. *Scale bars,* 10 μm. Data were evaluated using a one-way ANOVA (*, $p < 0.01$; $n = 3$ microscopic fields). *D* and *E,* CCDC120 knockdown also decreased the length of longest neurites and the total length of neurites. Data were evaluated using a one-way ANOVA (*, $p < 0.01$; $n = 50$ cells).

lysis buffer A and centrifuged. The supernatant was mixed with nickel-nitrilotriacetic acid resin. Bound His-tagged cytohesin-2 proteins were extensively washed with lysis buffer A containing 500 mM NaCl followed by lysis buffer containing 500 mM NaCl and 50 mM EDTA, and subsequently eluted with lysis buffer containing 10 mM imidazole (Nacalai Tesque), according to the manufacturer's protocol. The aliquot was stored at −80 °C until use.

siRNA Oligonucleotides—The 21-nucleotide siRNA duplexes were synthesized using Nippon EGT (Toyama, Japan). The specific target sequences were as follows: 5′-AAGATGGCAATGGGCAGGAAG-3′ for mouse cytohesin-2 siRNA and 5′-AAGCAGCAGAGGAAGACGTTC-3′ for mouse CCDC120 siRNA. The target sequence of the control *Photinus pyralis* luciferase siRNA was 5′-AAGCCATTCTATCCTCTAGAG-3′, which does not have significant homology to any mammalian gene sequences.

Cell Cultures—Mouse N1E-115 neuroblastoma cells and human embryonic kidney 293T cells were cultured on cell culture dishes at 37 °C in DMEM containing 10% heat-inactivated FBS, 50 units/ml penicillin, and 50 μg/ml streptomycin. For induction of differentiation, cells were cultured in normal medium in the absence of serum. Cells with processes longer than two cell bodies were counted as cells bearing neurites at 48 h after deprivation of serum.

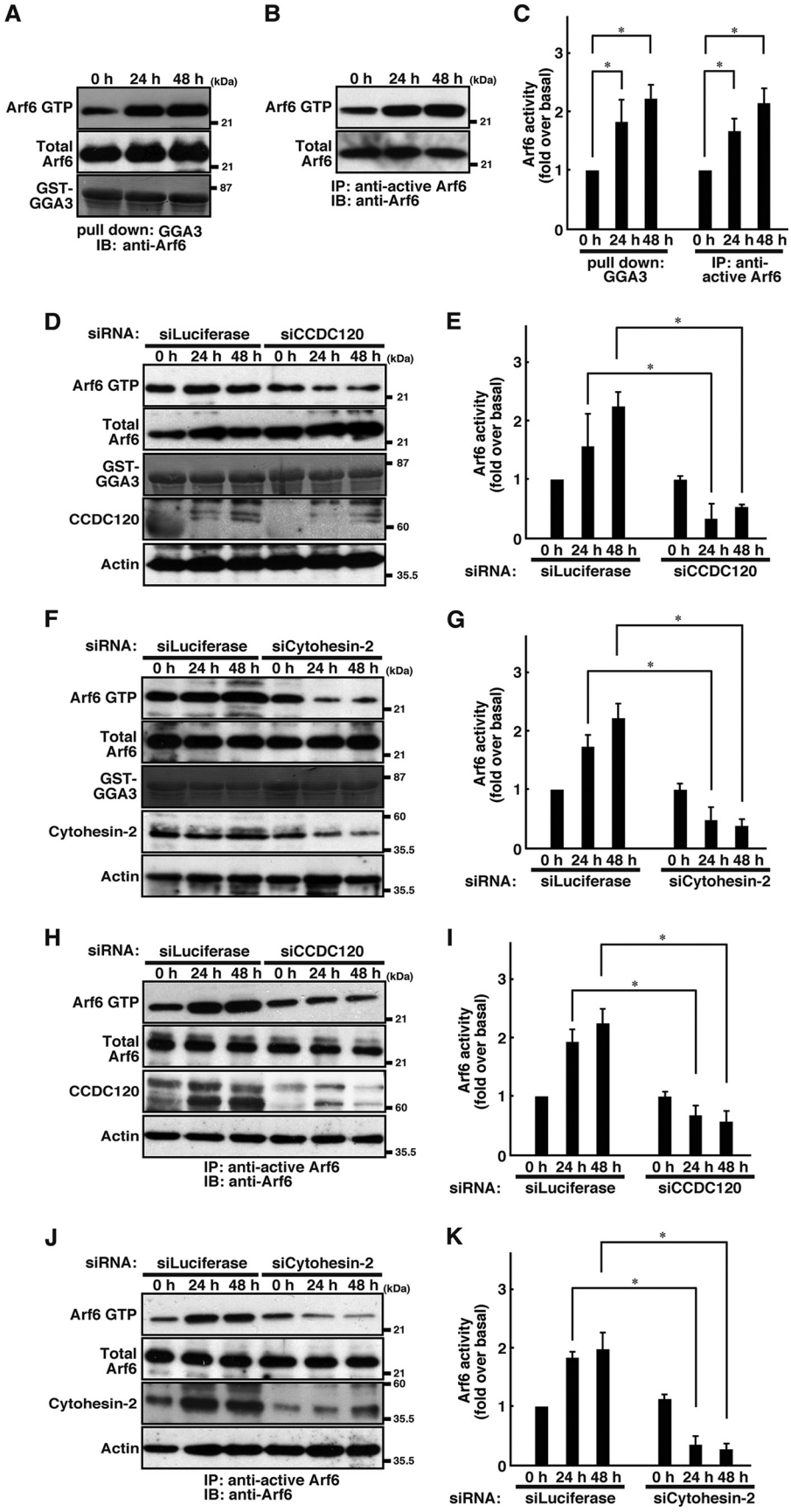
A
0 h 24 h 48 h (kDa)
Arf6 GTP
21
Total Arf6
21
GST-GGA3
87
pull down: GGA3
IB: anti-Arf6
B
0 h 24 h 48 h (kDa)
Arf6 GTP
21
Total Arf6
21
IP: anti-active Arf6
IB: anti-Arf6
C
Arf6 activity (fold over basal)
0 h 24 h 48 h
pull down: GGA3
0 h 24 h 48 h
IP: anti-active Arf6
D
siRNA: siLuciferase siCCDC120
0 h 24 h 48 h 0 h 24 h 48 h (kDa)
Arf6 GTP
21
Total Arf6
21
GST-GGA3
87
CCDC120
60
Actin
35.5
E
Arf6 activity (fold over basal)
0 h 24 h 48 h
siRNA: siLuciferase
0 h 24 h 48 h
siCCDC120
F
siRNA: siLuciferase siCytohesin-2
0 h 24 h 48 h 0 h 24 h 48 h (kDa)
Arf6 GTP
21
Total Arf6
21
GST-GGA3
87
Cytohesin-2
60
35.5
Actin
35.5
G
Arf6 activity (fold over basal)
0 h 24 h 48 h
siRNA: siLuciferase
0 h 24 h 48 h
siCytohesin-2
H
siRNA: siLuciferase siCCDC120
0 h 24 h 48 h 0 h 24 h 48 h (kDa)
Arf6 GTP
21
Total Arf6
21
CCDC120
60
Actin
35.5
IP: anti-active Arf6
IB: anti-Arf6
I
Arf6 activity (fold over basal)
0 h 24 h 48 h
siRNA: siLuciferase
0 h 24 h 48 h
siCCDC120
J
siRNA: siLuciferase siCytohesin-2
0 h 24 h 48 h 0 h 24 h 48 h (kDa)
Arf6 GTP
21
Total Arf6
21
Cytohesin-2
60
35.5
Actin
35.5
IP: anti-active Arf6
IB: anti-Arf6
K
Arf6 activity (fold over basal)
0 h 24 h 48 h
siRNA: siLuciferase
0 h 24 h 48 h
siCytohesin-2

Plasmid Transfection—N1E-115 cells were transfected with plasmid DNA using the Lipofectamine 2000 or Lipofectamine Plus transfection reagent (Invitrogen) according to the manufacturer's instructions. The medium was replaced 4 h after transfection. For 293T cells, plasmid DNAs were transfected using the CalPhos transfection reagent (TaKaRa Bio) according to the manufacturer's instructions. The medium was replaced 24 h after transfection.

siRNA Transfection—N1E-115 cells were transfected with siRNA oligonucleotides using the Lipofectamine 2000 transfection reagent. The medium was replaced 4 h after transfection.

Immunofluorescence—Cells were fixed in 4% paraformaldehyde in PBS, blocked with 20% heat-inactivated FBS in PBS, 0.05% Tween 20, incubated with each of the primary antibodies, and treated with fluorescence-labeled secondary antibodies in PBS containing 0.1% Tween 20. The coverslips were mounted onto slides with the Vectashield reagent (Vector Laboratories, Burlingame, CA) for observation using confocal microscopy. The confocal images were collected using an IX81 microscope with a laser-scanning FV1000 system (Olympus, Tokyo, Japan) and analyzed using FluoView software version 3.1 (Olympus).

Immunoblotting—Cells were lysed in lysis buffer B (50 mM HEPES-NaOH (pH 7.5), 20 mM $MgCl_2$, 150 mM NaCl, 1 mM dithiothreitol, 1 mM phenylmethanesulfonyl fluoride, 1 μg/ml leupeptin, 1 mM EDTA, 1 mM Na_3VO_4, 10 mM NaF, and 0.5% Nonidet P-40), and the lysates were centrifuged at 14,000 rpm for 10 min at 4 °C. The proteins in the supernatants were denatured in Laemmli sample buffer (0.4 M Tris-HCl (pH 6.8), 0.2 M dithiothreitol, 0.2% bromphenol blue, and 4% SDS) and then subjected to SDS-PAGE. The electrophoretically separated proteins were transferred to a PVDF membrane, blocked with the Blocking-One reagent (Nacalai Tesque, Kyoto, Japan), and immunoblotted with each of the primary antibodies and in turn with peroxidase-conjugated secondary antibodies. The bound antibodies were detected using the ChemiLumi-One reagent (Nacalai Tesque) or ECL select Western blotting detection system (GE Healthcare).

Immunoprecipitation—Cell lysates were mixed with protein G resin preadsorbed with each of the primary antibodies. The immune complexes were precipitated by centrifugation and washed three times using lysis buffer B. The immunoprecipitates were boiled in sample buffer and then separated on SDS-polyacrylamide gels. The bound proteins were detected using immunoblotting.

Assay for Arf6 Activity—To detect active GTP-bound forms of Arf6 in cell lysates, affinity precipitation was performed using GST-GGA3 (19, 20). The affinity-precipitated Arf6 was detected using Western blotting with an antibody against Arf6. For comparison of the amounts of recombinant GST-GGA3 proteins, GGA3 loaded under the same conditions was also stained with 0.25% Coomassie Brilliant Blue R-250.

Live Imaging—During the experiment, cells on a Cellview glass bottom cell culture dish (Greiner, Germany) were cultured in a small size CO_2 incubator (Tokai Hit, Shizuoka, Japan) containing 5% CO_2 at 37 °C and maintained in DMEM containing 50 units/ml penicillin and 50 μg/ml streptomycin. For live imaging, cells were scanned every 8 or 10 s for a duration of 4 min, using an IX81 microscope with a laser scanning FV1000 system. The confocal images were collected and analyzed through FluoView software version 3.1. The direction and the velocity of the vesicle's movement were analyzed by a kymograph illustrating using MetaMorph software (Molecular Devices, Sunnyvale, CA).

Statistical Analysis—Values shown represent the mean ± S.D. from separate experiments. A one-way ANOVA was used, followed by Fisher's protected least significant difference (PLSD) post hoc test (*, $p < 0.01$). The level of significance was set at $p < 0.05$.

RESULTS

Cytohesin-2 Interacts with CCDC120, Which Interacts through the CC1 Domain—The function of the protein CCDC120 was unknown, and it was identified as the binding partner of cytohesin-2 using comprehensive yeast two-hybrid analyses (21). To investigate whether CCDC120 interacts with cytohesin-2, we cotransfected the plasmids encoding FLAG-tagged cytohesin-2 and RFP-tagged CCDC120 into 293T cells. The lysate was used for an immunoprecipitation with an anti-FLAG antibody, and its immunocomplex was immunoblotted with an anti-RFP antibody. CCDC120 formed a complex with cytohesin-2 (Fig. 1*A*, *3rd lane*). In transfected 293T cells, some CCDC120 protein bands were observed using immunoblotting with an anti-RFP antibody. Because these protein bands were observed more in immunoblotting after immunoprecipitation, and when the bands were compared with those of a simple immunoblotting, they were thought to be CCDC120 degradation products. We next examined which CCDC120 region is involved in an interaction with cytohesin-2. To do this, we made a series of CCDC120 deletion mutants. CCDC120 (amino acids 1–350; Fig. 1*A*, *5th lane*), CCDC120 (amino acids 1–175; Fig. 1*B*, *3rd lane*), and CCDC120 (amino acids 1–92; Fig. 1*C*, *3rd lane*) were coimmunoprecipitated with

FIGURE 5. **CCDC120 and cytohesin-2 is involved in Arf6 activation in N1E-115 cells.** *A,* N1E-115 cells were treated with serum-free medium for 0, 24, or 48 h. After treatment, cells were lysed using lysis buffer. Cell lysates were affinity-precipitated with a recombinant GST-GGA3 and then immunoblotted with an anti-Arf6 antibody, respectively. *B,* N1E-115 cells were treated with serum-free medium for 0, 24, or 48 h. After treatment, cells were lysed using lysis buffer. Cell lysates were immunoprecipitated (*IP*) with an anti-active Arf6 antibody and then immunoblotted (*IB*) with an anti-Arf6 antibody. *C,* quantification of Arf6 activity from three independent experiments similar to that shown in *A* or *B*, respectively. Data were evaluated using a one-way ANOVA (*, $p < 0.01$; $n = 3$). *D* and *E,* N1E-115 cells were transfected with an siRNA for control luciferase or CCDC120 and allowed to differentiate for 0, 24, or 48 h. Arf6 activity was measured with affinity precipitation with GST-GGA3. The expression levels of Arf6, CCDC120, and actin and Coomassie staining of GST-GGA3 were also shown. *F* and *G,* N1E-115 cells transfected with an siRNA for control luciferase or cytohesin-2 was allowed to differentiate for 0, 24, or 48 h, and Arf6 activity was measured. Data were evaluated using a one-way ANOVA (*, $p < 0.01$; $n = 3$). *H* and *I,* N1E-115 cells were transfected with an siRNA for control luciferase or CCDC120 and allowed to differentiate for 0, 24, or 48 h. After treatment, cells were lysed using lysis buffer. Cell lysates were immunoprecipitated with an anti-active Arf6 antibody and then immunoblotted with an anti-Arf6 antibody. The expression levels of Arf6, CCDC120, and actin were shown. *J* and *K,* N1E-115 cells were transfected with an siRNA for control luciferase or cytohesin-2 and allowed to differentiate for 0, 24, or 48 h. After treatment, cells were lysed using lysis buffer. Cell lysates were immunoprecipitated with an anti-active Arf6 antibody and then immunoblotted with an anti-Arf6 antibody. The expression levels of Arf6, cytohesin-2, and actin are shown.

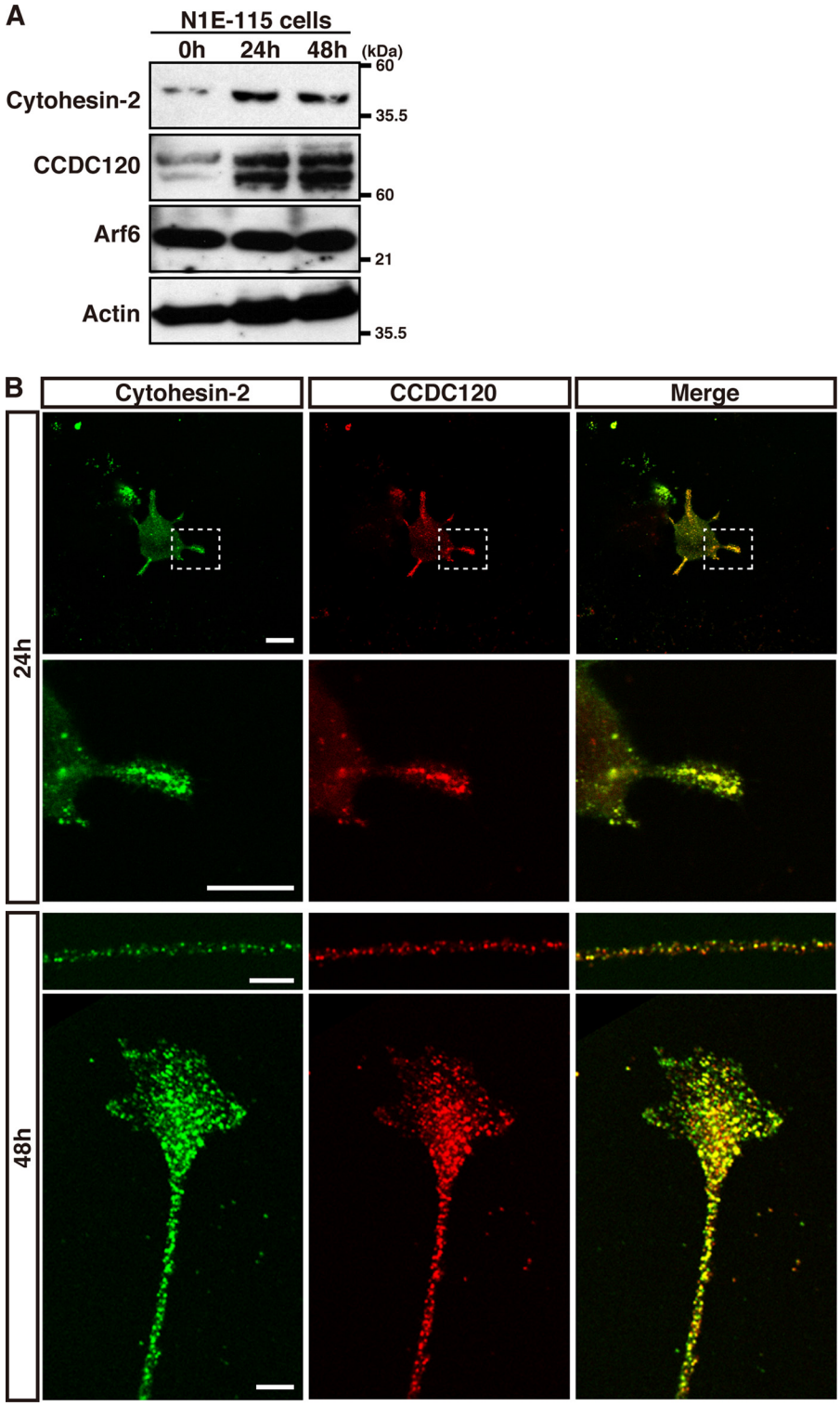

FIGURE 6. **CCDC120 colocalizes with cytohesin-2 in N1E-115 cells.** *A,* N1E-115 cells were allowed to differentiate for 0, 24, or 48 h, and the expression levels of cytohesin-2, CCDC120, Arf6, or actin were examined with immunoblotting using the respective antibodies. *B,* following induction of differentiation for 24 or 48 h, cells were coimmunostained with antibodies for cytohesin-2 (*green*) and CCDC120 (*red*). In the 24-h panels, enlarged photographs of *dotted squares* in *upper panels* are shown in *lower panels*. Colocalization of CCDC120 with cytohesin-2 was observed in both neurite shaft and growth cone areas. *Scale bars,* 10 μm.

cytohesin-2. Because secondary structural analysis using the COILS bioinformatics website predicts that CCDC120 has three CC domains, tentatively named CC1 (amino acids 33–70), CC2 (amino acids 104–137), and CC3 (amino acids 137–172) (Fig. 1*E*), CCDC120 (amino acids 1–92) corresponds to a region containing the CC1 domain. Following analyses using further deletion mutants, CCDC120 amino acids 31–70 were coimmunoprecipitated with cytohesin-2 (Fig. 1*D*, *7th lane*), revealing that the CCDC120 CC1 domain is responsible for the interaction with cytohesin-2.

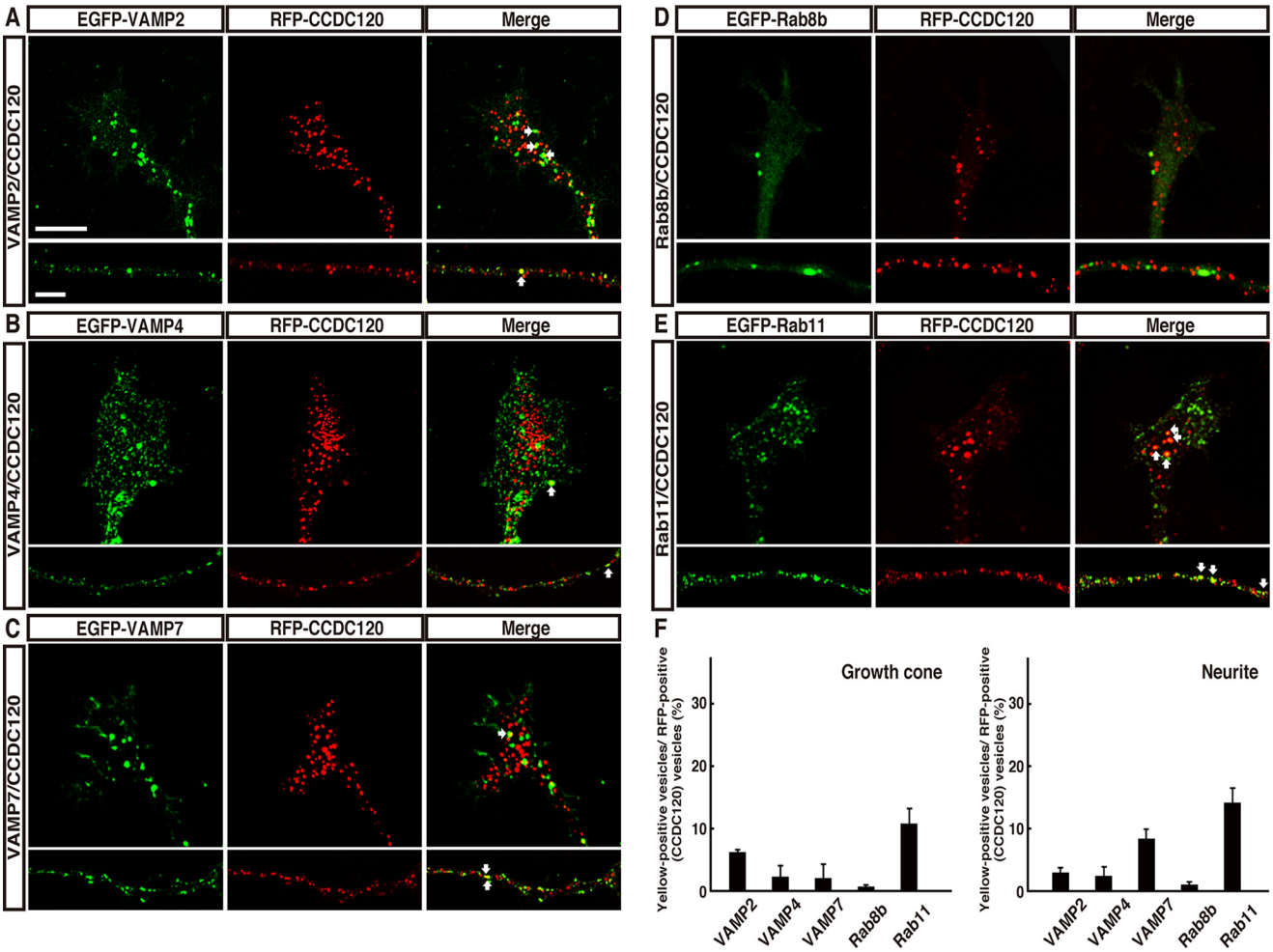

FIGURE 7. **Expression profiles of RFP-CCDC120 in N1E-115 cells.** N1E-115 cells were cotransfected with the plasmids encoding EGFP-VAMP2/synaptobrevin 2 (*A*), -VAMP4 (*B*), -VAMP7 (*C*), -Rab8b (*D*), -Rab11 (*E*), or RFP-CCDC120. Transfected cells were allowed to differentiate for 48 h, and vesicle-like structures containing EGFP-VAMPs/-Rabs (*green*) and RFP-CCDC120 (*red*) were observed in growth cones (*upper panels*) and neurites (*lower panels*) of N1E-115 cells, respectively. Colocalization with EGFP-VAMPs/-Rabs and RFP-CCDC120 are indicated by *white arrows*. *Scale bars,* 10 μm. *F,* at 48 h following differentiation, the ratios of colocalization between EGFP-Rabs/VAMPs and RFP-CCDC120 were measured in one growth cone (*left*) or neurite (*right*) (n = 15 neurites in each experiment).

Because coexpression of CCDC120 with cytohesin-2 inhibited CCDC120 degradation (Fig. 1*A*), we tested the possibility that cytohesin-2 inhibits ubiquitin modification of CCDC120 for the protein degradation system (22–24). CCDC120 was modified by HA-tagged ubiquitin in cells, and coexpression with cytohesin-2 resulted in inhibition of CCDC120 modification by ubiquitin (Fig. 1*F*). One of the reasons that cytohesin-2 inhibits CCDC120 degradation may be cytohesin-2 inhibition of CCDC120 ubiquitin modification.

N-terminal Region of Cytohesin-2 Interacts with CCDC120—To investigate which domains of cytohesin-2 interact with CCDC120, we generated a series of truncated cytohesin-2 mutants, tentatively named CC (amino acids 1–59), Sec7 (amino acids 60–254), PH+b (amino acids 255–400), PH (amino acids 255–384), and truncated cytohesin-2 (amino acids 60–384) (Fig. 2*A*). We cotransfected the plasmids encoding RFP-tagged CCDC120 and the respective FLAG-tagged domains and cytohesin-2 mutants into 293T cells. CCDC120 was coimmunoprecipitated with the CC domain (Fig. 2*B*, *2nd lane*) and weakly coimmunoprecipitated with the Sec7 domain and truncated cytohesin-2 (amino acids 60–384) (Fig. 2, *B*, *3rd lane,* and *C*, *3rd lane*), revealing that the cytohesin-2 CC domain provides the primary interaction region with CCDC120.

CCDC120 Directly Binds to Cytohesin-2—To determine whether CCDC120 directly binds to cytohesin-2, recombinant GST-tagged CC1 domain proteins of CCDC120 were produced in *E. coli* (Fig. 3*A*). His-tagged cytohesin-2 proteins were also produced and purified using *E. coli*. The GST-tagged CC1 domain of CCDC120 proteins exhibited a specific binding with immobilized His-cytohesin-2 proteins, but this was not observed in control GST proteins. Scatchard analysis for the interaction between the CC1 domain and cytohesin-2 revealed its binding dissociation constant (K_d) of 0.28 ± 0.033 μM (Fig. 3*B*), which suggests direct binding.

Cytohesin-2-binding Protein CCDC120 Regulates Neurite Growth in N1E-115 Cells—N1E-115 cells have been used as a good model to study neurite outgrowth, because N1E-115 cells can form comparatively long neurites (15, 25–29). N1E-115 cells normally undergo proliferation in the presence of 10% FBS. Following induction of differentiation by serum depriva-

tion, 30–40% of cells exhibit phenotypes bearing extended neurites at 48 h (16).

To explore the role of the cytohesin-2-binding protein CCDC120 in N1E-115 cells, we transfected each CCDC120 siRNA oligonucleotide or control luciferase into N1E-115 cells. Immunoblotting showed that CCDC120 expression levels were specifically knocked down by CCDC120 siRNA transfection, whereas the expression levels of control actin were unaffected (Fig. 4*A*). Following induction of differentiation, transfection of CCDC120 siRNA into N1E-115 cells decreased the length

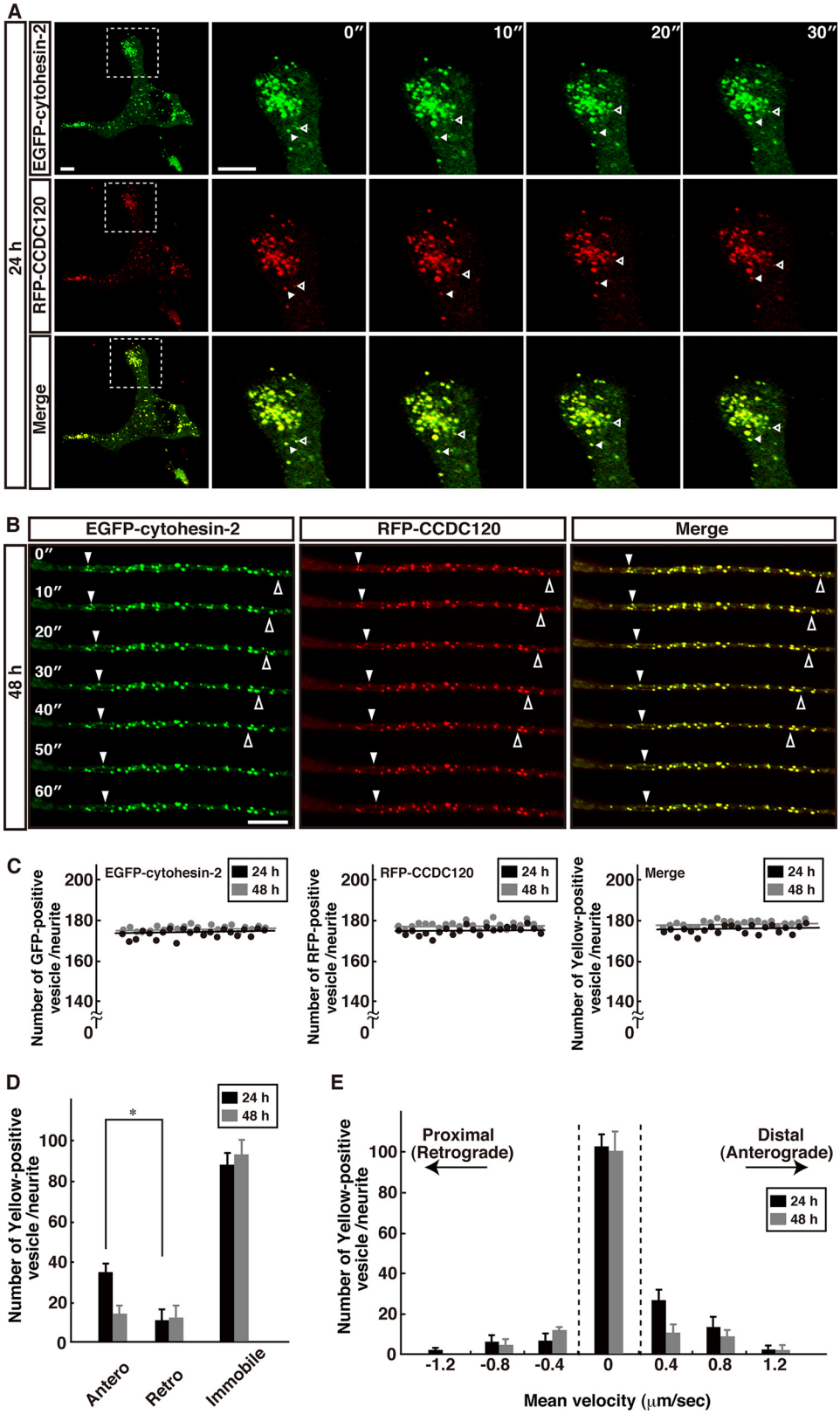

of the longest neurites by ~70% compared with transfection of control siRNA (Fig. 4, *B* and *D*). Similarly, transfection of CCDC120 siRNA decreased the total length of neurites by ~50% (Fig. 4, *B* and *E*). Knockdown of CCDC120 also decreased the numbers of cells with single neurites by ~0.4-fold (13 ± 0.29 in CCDC120 knockdown compared with 30 ± 0.94 in control knockdown) and increased the numbers of cells with multiple neurites (≥2 neurites) by ~2.6-fold (23 ± 0.78 in CCDC120 knockdown compared with 8.8 ± 0.43 in control knockdown) (Fig. 4, *B* and *C*), suggesting that CCDC120 mediates neurite growth by controlling the neurite length and number.

CCDC120 and Cytohesin-2 Regulate Arf6 Activation in Differentiating N1E-115 Cells—In our previous report, Arf6 activity significantly increased during neurite outgrowth in N1E-115 cells (16). Similarly, we performed an affinity precipitation as pulldown using recombinant GST-tagged N-terminal domain of GGA3, which specifically binds to the active GTP-bound form of Arf6. Increasing Arf6 activity was detected by pulldown assay (Fig. 5, *A* and *C*), consistent with the results from an immunoprecipitation assay using anti-active Arf6 (Fig. 5, *B* and *C*) in growing N1E-115 cells. Because cytohesin-2 is a GEF for Arf6 (12, 13), we examined whether CCDC120 is involved in Arf6 activation in N1E-115 cells. Under control siRNA transfection conditions, GTP-bound Arf6 was observed to be affinity-precipitated with GST-GGA3 at 24 or 48 h following induction of differentiation, whereas transfection with CCDC120 siRNA inhibited Arf6 activation (Fig. 5, *D* and *E*), indicating that CCDC120 is required for Afr6 activation in differentiation. We also confirmed that knockdown of cytohesin-2 inhibited Arf6 activation under the experimental conditions (Fig. 5, *F* and *G*) (16). Similar knockdown effects were also shown by immunoprecipitation assay using an anti-active Arf6 antibody (Fig. 5, *H–K*).

CCDC120 and Cytohesin-2 Are Present in Punctate Structures in Growing Neurites in N1E-115 Cells—As shown in Fig. 6*A*, CCDC120 expression levels increased as differentiation proceeded in N1E-115 cells. We also confirmed that expression levels of cytohesin-2, but not Arf6 and control actin proteins, increased following induction of differentiation (16). Because CCDC120 expression profiles are similar to those of cytohesin-2, we tested the possibility that CCDC120 may be associated with cytohesin-2 in subcellular components. At 24 h after induction of differentiation, CCDC120 and cytohesin-2 were observed in punctate structures throughout the growing neurites (Fig. 6*B*, *upper six panels*). At 48 h after induction of differentiation, colocalization of CCDC120 with cytohesin-2 was also observed in both neurite shaft and growth cone areas (Fig. 6*B*, *lower six panels*).

CCDC120- and Cytohesin-2-containing Vesicles Are Transported Along Neurites in N1E-115 Cells—To identify the vesicle-like structures containing CCDC120, we cotransfected RFP-CCDC120, EGFP-VAMPs (VAMP2/synaptobrevin2, VAMP4, and VAMP7), or EGFP-Rabs (Rab8b or Rab11), together with RFP-CCDC120, into N1E-115 cells. At 48 h after induction of differentiation, the ratios of colocalization of both RFP-CCDC120 and EGFP fusion proteins in growth cone and neurites of N1E-115 cells were calculated from fluorescence images (Fig. 7, *A–E*). Because these values were about 20% at most (Fig. 7*F*), the vesicle-like structures containing CCDC120 was very partially colocalized to these endosomal vesicles. These results suggest that CCDC120 can be present in both anterograde and retrograde moving vesicles along neurites. Next, to visualize movement of cytohesin-2 and CCDC120 in neurites, we transfected the plasmid encoding EGFP-cytohesin-2 and RFP-CCDC120 into N1E-115 cells and observed their movement using time-lapse fluorescence microscopy. At both 24 and 48 h after induction of differentiation, green fluorescence-positive EGFP-cytohesin-2 and red fluorescence-positive RFP-CCDC120 were localized in vesicle-like structures along neurites (Fig. 8, *A–C*). They were also colocalized in vesicle-like structures, where many of the yellow fluorescence-positive colocalization signals for EGFP and RFP were observed (Fig. 8, *A–C*), which is consistent with the immunofluorescence results from Fig. 6*B*. 24 h after induction of differentiation, vesicles containing EGFP-cytohesin-2 and RFP-CCDC120 moved in the anterograde rather than retrograde direction along growing neurites, although ~50% of vesicles were immobile (Fig. 8*D*; supplemental Movie 1), suggesting that when neurites begin outgrowth, their vesicles preferentially move in the anterograde direction. In contrast, at 48 h after induction of differentiation, the vesicles moved along neurites almost equally in the anterograde and retrograde directions (Fig. 8*D*; supplemental Movie 2). As shown in Fig. 7*E*, the histogram of mean velocity revealed that vesicles transported in both anterograde and retrograde directions move at a broad range of average transport rates along neurites (Fig. 8*E*).

Cytohesin-2 Is Recruited to Vesicles through the CC1 Domain of CCDC120—Because cytohesin-2 binds to CCDC120, we tested whether CCDC120 has the ability to regulate the translocation of cytohesin-2. We thus made an RFP-tagged cytohesin-2-binding CC1 domain-deficient CCDC120 mutant (RFP-CCDC120-ΔCC1) (Fig. 9*A*) and cotransfected the wild type or mutant CCDC120 construct with FLAG-cytohesin-2 into 293T

FIGURE 8. **Vesicle-like structures containing cytohesin-2 and CCDC120 are transported along neurites in N1E-115 cells.** N1E-115 cells were cotransfected with the plasmids encoding EGFP-cytohesin-2 and RFP-CCDC120 and were allowed to differentiate for 24 or 48 h. *A* and *B,* at 24 or 48 h following differentiation, a live image in a neurite was captured for 4 min, and representative images for 30 or 60 s are shown, respectively. Vesicle-like structures containing EGFP-cytohesin-2 (*green*) and RFP-CCDC120 (*red*) were observed in neurites. *Closed* and *open arrowheads* indicate representative retrograde and anterograde movements, respectively. In 24-h panels, enlarged photographs of *dotted squares* are shown as live images. *Scale bars,* 5 μm (*A*) or 10 μm (*B*). *C,* at 24 or 48 h following differentiation, the number of green fluorescence-positive cytohesin-2-containing vesicles, red fluorescence-positive CCDC120-containing vesicles, and merged yellow fluorescence-positive vesicles in one neurite was counted ($n = 22$ neurites in each experiment). Almost all vesicles contained both cytohesin-2 and CCDC120. *D,* at 24 or 48 h following differentiation, the number of yellow fluorescence-positive or immobile vesicles moving in anterograde or retrograde directions were counted in one neurite ($n = 20$ neurites in each experiment). Data were evaluated using a one-way ANOVA (*, $p < 0.01$). *E,* velocity distribution of yellow fluorescence-positive vesicles moving in anterograde or retrograde directions or immobile vesicles in one neurite is shown ($n = 25$ neurites in each experiment).

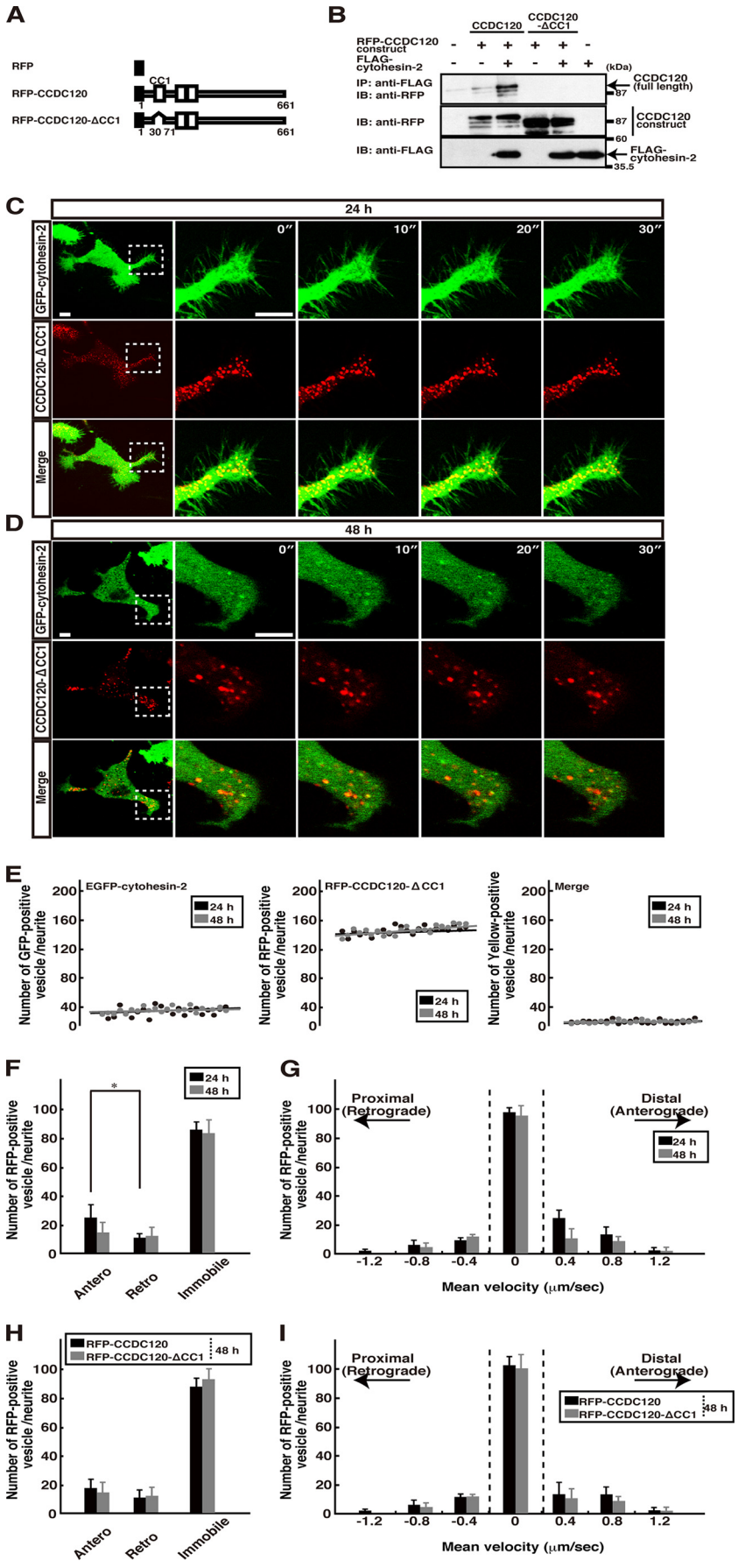
A
RFP
CC1
RFP-CCDC120
1
661
RFP-CCDC120-ΔCC1
1 30 71
661
B
CCDC120
CCDC120 -ΔCC1
RFP-CCDC120 construct
FLAG-cytohesin-2
(kDa)
IP: anti-FLAG
IB: anti-RFP
CCDC120 (full length)
87
IB: anti-RFP
87
CCDC120 construct
60
IB: anti-FLAG
FLAG-cytohesin-2
35.5
C
24 h
GFP-cytohesin-2
CCDC120-ΔCC1
Merge
0″
10″
20″
30″
D
48 h
GFP-cytohesin-2
CCDC120-ΔCC1
Merge
0″
10″
20″
30″
E
EGFP-cytohesin-2
Number of GFP-positive vesicle /neurite
200
160
120
80
40
0
24 h
48 h
RFP-CCDC120-ΔCC1
Number of RFP-positive vesicle /neurite
Merge
Number of Yellow-positive vesicle /neurite
F
Number of RFP-positive vesicle /neurite
100
80
60
40
20
0
*
24 h
48 h
Antero
Retro
Immobile
G
Proximal (Retrograde)
Distal (Anterograde)
Number of RFP-positive vesicle /neurite
-1.2
-0.8
-0.4
0
0.4
0.8
1.2
Mean velocity (μm/sec)
H
RFP-CCDC120
RFP-CCDC120-ΔCC1
48 h
Number of RFP-positive vesicle /neurite
Antero
Retro
Immobile
I
Proximal (Retrograde)
Distal (Anterograde)
Number of RFP-positive vesicle /neurite
Mean velocity (μm/sec)

cells. The wild type coimmunoprecipitated with cytohesin-2, but the mutant did not (Fig. 9*B*), confirming our data that the CC1 domain is required for coimmunoprecipitation with cytohesin-2.

We next performed a time-lapse fluorescence microscopy at 24 or 48 h after induction of differentiation in N1E-115 cells. Although RFP-CCDC120-ΔCC1 was localized in vesicle-like structures, EGFP-cytohesin-2 was distributed throughout the cytoplasmic regions (Fig. 9, *C* and *D,* and supplemental Movies 3 and 4), indicating that CCDC120 determines cellular cytohesin-2 localization. CCDC120-ΔCC1- and cytohesin-2-containing vesicles amounted to less than 5% of all vesicles (Fig. 9*E*). Although ~80% of CCDC120-ΔCC1-containing vesicles were immobile, the mobile vesicles moved in the anterograde and retrograde directions at a broad range of average transport rates along neurites (Fig. 9, *F–I*).

Arf6 Activation Requires the Interaction between CCDC120 and Cytohesin-2—We next examined whether the interaction between CCDC120 and cytohesin-2 is required for Arf6 activation. We transfected the plasmid encoding either RFP-CCDC120 or RFP-CCDC120-ΔCC1 into N1E-115 cells and immunostained it with an anti-active Arf6 antibody at 48 h after induction of differentiation. The wild type CCDC120 signals were colocalized with signals showing active Arf6 in vesicle-like structures in both neurite shaft and growth cone areas (Fig. 10, *A*, *upper six panels,* and *B*). The signals of CCDC120-ΔCC1 were detected as punctate structures in immature neurites; however, active Arf6 signals promptly decreased and rather appeared to be diffused in cells (Fig. 10, *A*, *lower six panels,* and *B*). These results are consistent with the results that transfection of CCDC120-ΔCC1 diffuses EGFP-cytohesin-2 in the cytoplasmic regions.

Neurite Growth Requires the Interaction between CCDC120 and Cytohesin-2—To clarify whether the interaction between CCDC120 and cytohesin-2 is required for neurite growth, the plasmid encoding RFP-CCDC120, RFP-CCDC120-ΔCC1, or control RFP was cotransfected with each siRNA for CCDC120 or control luciferase into N1E-115 cells. CCDC120 siRNA transfection decreased the length of the longest neurites and the total length of neurites. It also decreased the numbers of cells with a single neurite and increased the numbers of cells with multiple neurites (Fig. 11*A*, *lower 2nd panel* compared with *upper 2nd panel*). Under the same CCDC120 siRNA transfection condition, cotransfection of CCDC120-ΔCC1 did not reverse these phenotypes (Fig. 11*A*, *lower 4th panel*), similar to the phenotypes observed in CCDC120-ΔCC1 cotransfection under the control of siRNA transfection conditions (Fig. 11*A*, *upper 4th panel*), suggesting that CCDC120-ΔCC1 may also act as the dominant-negative in neurite growth. However, wild type CCDC120 cotransfection under CCDC120 siRNA transfection conditions reversed the effects of CCDC120 siRNA and exhibited a seemingly normal phenotype (Fig. 11*A*, *lower 6th panel*). These statistical data are summarized in Fig. 11, *B* (longest neurite length), *C* (total neurite length), and *D* (neurite number). Collectively, the interaction of cytohesin-2 with CCDC120 participates in determining cytohesin-2 localization in vesicle-like structures to regulate Arf6 activation and neurite growth.

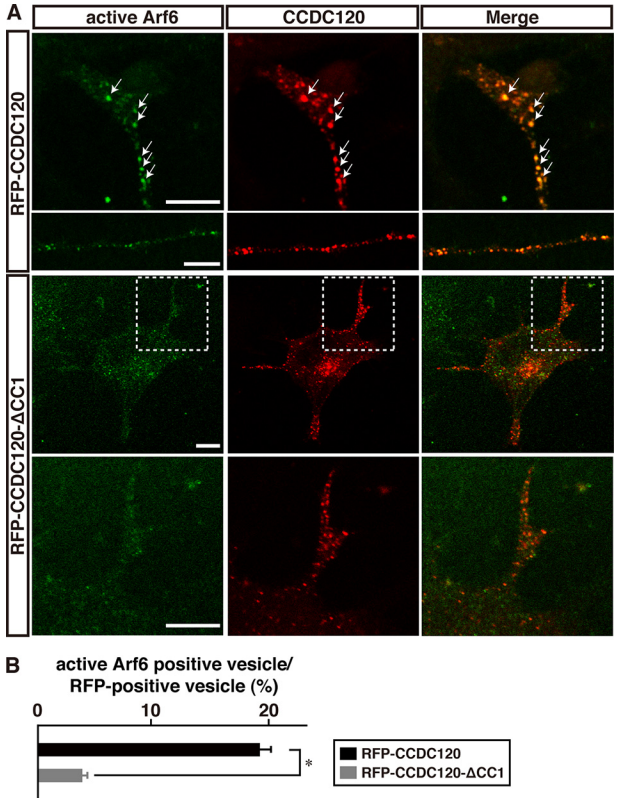

FIGURE 10. **Interaction between CCDC120 and cytohesin-2 is required for both neurite growth and Arf6 activation.** *A,* at 48 h following differentiation, N1E-115 cells expressing RFP-CCDC120 or RFP-CCDC120-ΔCC1 were immunostained with an anti-active Arf6 antibody. In RFP-CCDC120-ΔCC1 panels, enlarged photographs of *dotted squares* in *upper panels* are shown in the *lower panels*. *Scale bars,* 5 μm. *B,* percentage of active Arf6-positive vesicles in CCDC120-positive vesicles in neurites is shown ($n = 25$ neurites in each experiment). Data were evaluated using a one-way ANOVA (*, $p < 0.01$).

FIGURE 9. **CCDC120 is required for localization of cytohesin-2 in N1E-115 cells.** *A,* schematic structure of RFP-CCDC120 and RFP-CCDC120-ΔCC1 that are incapable of binding to cytohesin-2 is shown (*numbers* show amino acid structures). *B,* 293T cells were transfected with the plasmids encoding either RFP-CCDC120 or RFP-CCDC120-ΔCC1 together with FLAG-cytohesin-2. The immunoprecipitates (*IP*) with an anti-FLAG antibody were immunoblotted (*IB*) with an anti-RFP antibody. Expression levels of transfected plasmids are shown. *C* and *D,* N1E-115 cells were cotransfected with the plasmids encoding EGFP-cytohesin-2 and RFP-CCDC120-ΔCC1 and were allowed to differentiate for 24 (*C*) or 48 h (*D*). These live images in a neurite were captured for 4 min, and representative images for 30 s are shown. Vesicle-like structures containing RFP-CCDC120-ΔCC1 (*red*) were observed in neurites, whereas EGFP-cytohesin-2 (*green*) was widely localized in the cytoplasmic regions. Enlarged photographs of *dotted squares* are shown as live images. *Scale bars,* 5 μm. *E,* at 24 or 48 h following differentiation, the number of green fluorescence-positive cytohesin-2-containing vesicles, red fluorescence-positive CCDC120-ΔCC1-containing vesicles, and yellow fluorescence-positive vesicles in one neurite were counted ($n = 22$ neurites in each experiment). *F,* at 24 or 48 h following differentiation, the number of yellow fluorescence-positive or immobile vesicles moving in anterograde (*Antero*) or retrograde (*Retro*) directions were counted in one neurite ($n = 20$ neurites in each experiment). Data were evaluated using a one-way ANOVA (*, $p < 0.01$). *G,* velocity distribution of yellow fluorescence-positive vesicles moving in anterograde or retrograde directions or immobile vesicles in one neurite is shown ($n = 24$ neurites in each experiment). *H,* number of RFP-CCDC120 or CCDC120-ΔCC1-containing vesicles moving in anterograde or retrograde directions or immobile vesicles in one neurite were counted ($n = 28$ neurites in each experiment). *I,* velocity distribution of RFP-CCDC120 or CCDC120-ΔCC1-containing vesicles moving in anterograde or retrograde directions or immobile vesicles in one neurite are shown ($n = 33$ neurites in each experiment).

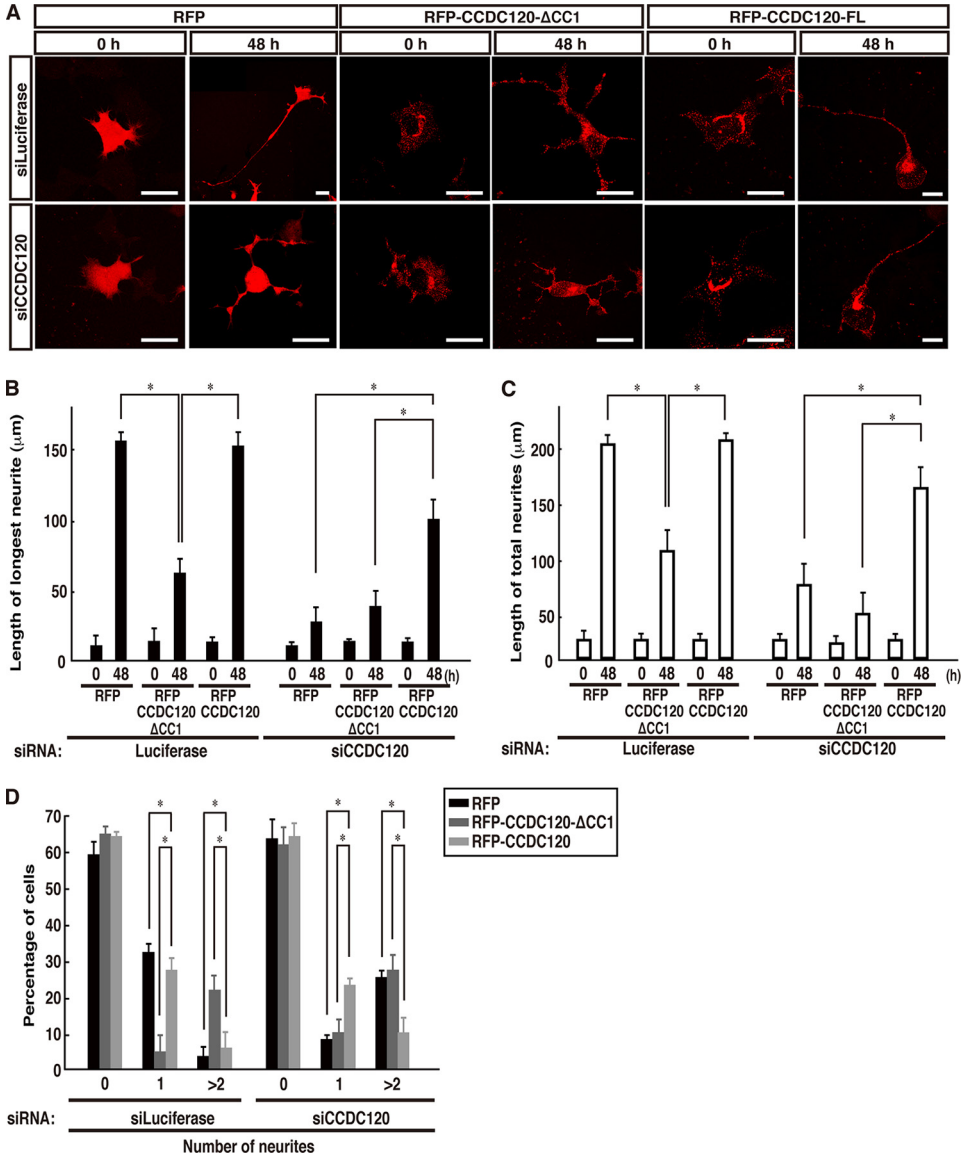

FIGURE 11. **Interaction of cytohesin-2 with CCDC120 is required for neurite growth.** *A,* N1E-115 cells were cotransfected with the plasmid encoding RFP, RFP-CCDC120, or RFP-CCDC120-ΔCC1 and an siRNA for control luciferase or CCDC120. Representative images are also shown at 0 or 48 h following induction of differentiation. *Scale bars,* 10 μm. The length of the longest neurites (*B*) and the total number of neurites (*C*) per cell were measured ($n = 54$ cells). *D*, number of neurites in each cell was counted and shown as the percentage ($n = 3$ microscopic fields). Data were evaluated using a one-way ANOVA (*, $p < 0.01$).

DISCUSSION

Neuronal morphological changes include neurite outgrowth, extension, axon guidance, branching, synapse connection, and neuronal network formation. It is well established that the initial events of these morphological changes are composed of the complex signaling mechanisms involving Rho and Ras families of small GTPases (2–4). Increasing evidence illustrates that small GTPases of the Arf family and the downstream effectors also regulate morphological changes in neuronal cells and increase the complexity of signaling mechanisms underlying neuronal morphological changes (30). However, comparatively less is known about regulation and localization of molecules controlling the Arf activity in cells. We previously reported the critical role of cytohesin-2 in neurite outgrowth in N1E-115 cells (15, 16). Here, we report that Arf6-GEF cytohesin-2 binds to a protein, CCDC120, which is a previously unknown function, and localizes on vesicles containing CCDC120 to be transported along neurites in differentiating N1E-115 cells. The importance of CCDC120 in cytohesin-2 regulation is supported by inhibition of neurite growth and Arf6 activation in response to CCDC120 knockdown. When neurites begin to extend, vesicles containing CCDC120 and cytohesin-2 are transported in a more anterograde direction. As neurites extend, anterograde vesicle transport decreases. Indeed, cytohesin-2 localization on vesicles containing CCDC120 is blocked by CCDC120 knockdown. Reintroduction of the wild type construct into CCDC120 knockdown background reverses blunted neurite growth, whereas that of the cytohesin-2-binding CC1 region-deficient CCDC120 construct fails to reverse it. Thus, cytohesin-2 is transported by vesicles containing CCDC120 along neurites and mediates neurite growth. We clarify for the first time the molecule required for transporting Arf6-GEF.

It is well known that adaptor and/or anchor proteins determine the localization of GEFs for small Rab family GTPases, which are essential for intracellular membrane transport. For example, a tetanus neurotoxin-insensitive vesicle-associated membrane protein (VAMP7/TI-VAMP) interacts with the Vps domain and ankyrin repeat-containing protein (Varp), which is characterized as a GEF for small GTPase Rab21, and they partially colocalize in the cell body, neurite shafts, and the peripheral region of neurites (31). VAMP7 and Varp-containing vesicles exhibit anterograde and retrograde transport along neurites in hippocampal neurons. The anterograde transport of the vesicles from trans-Golgi network to the cell surface mediates the kinesin superfamily 5A (KIF5A) motor proteins in neurons, and it is important for neurite differentiation and polarization (32). There is another example in exocytic membrane trafficking process from the Golgi. Rabin8, which is a GEF for Rab8, regulates vesicle trafficking containing the retinal photoreceptor rhodopsin from trans-Golgi network to the cilia base (33, 34). Rabin8 is recruited to Golgi-derived vesicles by Rab11 as a Golgi-localized anchor protein (35, 36) at the early stage of primary ciliogenesis. These mechanisms suggest an hypothesis that CCDC120 may bind to vesicles through presumably adaptor(s) to transport cytohesin-2 along neurites. Further studies investigating CCDC120-binding protein(s) will clarify how CCDC120 determines cytohesin-2 localization.

Morphological changes in neuronal cells involve some Arf6-GEFs, which are composed of the enhancer EFA6 ((also known as pleckstrin and Sec7 domain containing) and brefeldin A-resistant Arf-GEF (BRAG (also known as the IQ motif and SEC7 domain-containing protein, IQSEC) family proteins. EFA6A, EFA6B, EFA6C, and EFA6D constitute EFA6 family members (37–39). Among them, EFA6A and EFA6C are predominantly expressed in the central nervous system, whereas EFA6B and EFA6D are widely distributed in various tissues (39, 40). EFA6A is abundantly expressed in hippocampal neurons and regulates dendrite formation (41). The short variant of EFA6A (EFA6As) is known to participate in regulating dendrite branching during central nervous system development (42). BRAG1, BRAG2/GEP100, and BRAG3 constitute the BRAG family members. Although all BRAG members are expressed in the central nervous system, each BRAG member likely exhibits an individual expression pattern. BRAG1 and BRAG3 are widely distributed in the central nervous system (43) and BRAG2 is abundantly expressed in the hippocampus (44) and cancer cells (45). Because the EFA6 and BRAG members contain one or multiple CC domains (10), these GEFs may interact with CCDC120 in neuronal cells and may act together with the EFA6 and BRAG members to mediate their morphological changes.

Thus far, many cytohesin family-binding proteins have been identified to modulate cytohesin activities and signaling through cytohesins in various types of cells. The CC domain in cytohesins is characterized to provide a binding site with other CC domain-containing proteins. The CC domains include the Grp1 signaling partner 1 (GRSP1)/mKIAA1013 (46, 47), the Grp1-associated scaffold protein (GRASP)/tamalin (48), cytohesin-associated scaffold protein (CASP)/Cybr/cytohesin-interacting protein (CYTIP) (49–51), interaction protein for cytohesin exchange factor 1 (IPCEF1)/KIAA0403 (52, 53), FERM domain containing 4A (FRMD4A) (54), connector enhancer of KSR 1 (CNK1) (55), and the small GTPase family member Arl4D (56, 57). Although CASP and FRMD4A bind very specifically with cytohesin-1, GRSP1, GRASP, IPCEF, CNK1, and Arl4D bind possibly to all cytohesin family proteins (56). It is clear that cytohesin-2 binds to CCDC120 to be transported by vesicles containing CCDC120 along neurites, but one or some of these binding proteins may also help cytohesin-2 to localize along neurites.

Arf6 is well established to stimulate the activities of phosphatidylinositol-4-phosphate 5-kinases and phospholipase D isoenzymes. These enzymes generate phosphoinositides and phospholipids as the products, causing cell morphological changes. Therefore, these lipid-modifying enzymes may act as the effector of Arf6 in the neuronal cell signaling pathway at CCDC120-containing vehicles and/or final destinations where cytohesin-2 may localize. In the normal process outgrowth condition in N1E-115 cells, cytohesin-2 is localized in CCDC120-positive vesicles where the cytohesin-2 target molecule Arf6 is colocalized. In contrast, when CCDC120 is knocked down in cells, cytohesin-2 is dispersed throughout the cytoplasmic region. CCDC120 knockdown also inhibits process outgrowth in N1E-115 cells. CCDC120 may allow cytohesin-2 to localize to regulate promising Arf6 activation in certain vesicles but not the whole cytoplasmic region, which is probably required for extending processes.

Here, we show that cytohesin-2 is transported by vesicles containing CCDC120 along the neurites to mediate neurite growth. Further studies along this line will allow us to understand the detailed mechanisms of how CCDC120 localizes cytohesin-2 in vesicles, and also why cytohesin-2-binding protein CCDC120 is required for neurite growth. This may require further studies to clarify how the activity of cytohesin-2 is spatiotemporally regulated by kinases such as PKC (14, 58).

Acknowledgments—We thank Drs. Y. Matsubara and H. Saito (National Research Institute for Child Health and Development) for helpful discussions. We also thank Dr. J. Smith for English sentence review.

REFERENCES

1. Craig, A. M., and Banker, G. (1994) Neuronal polarity. *Annu. Rev. Neurosci.* **17,** 267–310
2. da Silva, J. S., and Dotti, C. G. (2002) Breaking the neuronal sphere: regulation of the actin cytoskeleton in neuritogenesis. *Nat. Rev. Neurosci.* **3,** 694–704
3. Govek, E. E., Newey, S. E., and Van Aelst, L. (2005) The role of the Rho GTPases in neuronal development. *Genes Dev.* **19,** 1–49
4. Arimura, N., and Kaibuchi, K. (2007) Neuronal polarity: from extracellular signals to intracellular mechanisms. *Nat. Rev. Neurosci.* **8,** 194–205
5. Park, H., and Poo, M. M. (2013) Neurotrophin regulation of neural circuit development and function. *Nat. Rev. Neurosci.* **14,** 7–23
6. Bray, D. (1970) Surface movements during the growth of single explanted neurons. *Proc. Natl. Acad. Sci. U.S.A.* **65,** 905–910
7. Pfenninger, K. H. (2009) Plasma membrane expansion: a neuron's Herculean task. *Nat. Rev. Neurosci.* **10,** 251–261
8. D'Souza-Schorey, C., and Chavrier, P. (2006) ARF proteins: roles in membrane traffic and beyond. *Nat. Rev. Mol. Cell Biol.* **7,** 347–358
9. Kahn, R. A., Cherfils, J., Elias, M., Lovering, R. C., Munro, S., and Schurmann, A. (2006) Nomenclature for the human Arf family of GTP-binding

proteins: ARF, ARL, and SAR proteins. *J. Cell Biol.* **172,** 645–650
10. Casanova, J. E. (2007) Regulation of Arf activation: the Sec7 family of guanine nucleotide exchange factors. *Traffic* **8,** 1476–1485
11. Donaldson, J. G., and Jackson, C. L. (2011) ARF family G proteins and their regulators: roles in membrane transport, development, and disease. *Nat. Rev. Mol. Cell Biol.* **12,** 362–375
12. Chardin, P., Paris, S., Antonny, B., Robineau, S., Béraud-Dufour, S., Jackson, C. L., and Chabre, M. (1996) A human exchange factor for ARF contains Sec7- and pleckstrin-homology domains. *Nature* **384,** 481–484
13. Frank, S., Upender, S., Hansen, S. H., and Casanova, J. E. (1998) ARNO is a guanine nucleotide exchange factor for ADP-ribosylation factor 6. *J. Biol. Chem.* **273,** 23–27
14. DiNitto, J. P., Delprato, A., Gabe Lee, M. T., Cronin, T. C., Huang, S., Guilherme, A., Czech, M. P., and Lambright, D. G. (2007) Structural basis and mechanism of autoregulation in 3-phosphoinositide-dependent Grp1 family Arf GTPase exchange factor. *Mol. Cell* **28,** 569–583
15. Yamauchi, J., Miyamoto, Y., Torii, T., Mizutani, R., Nakamura, K., Sanbe, A., Koide, H., Kusakawa, S., and Tanoue, A. (2009) Valproic acid-inducible Arl4D and cytohesin-2/ARNO, acting through the downstream Arf6, regulate neurite outgrowth in N1E-115 cells. *Exp. Cell Res.* **315,** 2043–2052
16. Torii, T., Miyamoto, Y., Nakamura, K., Maeda, M., Yamauchi, J., and Tanoue, A. (2012a) Arf6 guanine-nucleotide exchange factor, cytohesin-2, interacts with actinin-1 to regulate neurite extension. *Cell. Signal.* **24,** 1872–1882
17. Torii, T., Miyamoto, Y., Sanbe, A., Nishimura, K., Yamauchi, J., and Tanoue, A. (2010) Cytohesin-2/ARNO, through its interaction with focal adhesion adaptor protein paxillin, regulates preadipocyte migration via the downstream activation of Arf6. *J. Biol. Chem.* **285,** 24270–24281
18. Torii, T., Miyamoto, Y., Nishimura, K., Nakamura, K., Maeda, M., Tanoue, A., and Yamauchi, J. (2012) The polybasic region of cytohesin-2 determines paxillin binding specificity to mediate cell migration. *Adv. Biol. Chem.* **2,** 291–300
19. Boman, A. L., Zhang, C. j., Zhu, X., and Kahn, R. A. (2000) A family of ADP-ribosylation factor effectors that can alter membrane transport through the trans-Golgi. *Mol. Biol. Cell* **11,** 1241–1255
20. Dell'Angelica, E. C., Puertollano, R., Mullins, C., Aguilar, R. C., Vargas, J. D., Hartnell, L. M., and Bonifacino, J. S. (2000) GGAs: a family of ADP ribosylation factor-binding proteins related to adaptors and associated with the Golgi complex. *J. Cell Biol.* **149,** 81–94
21. Rual, J. F., Venkatesan, K., Hao, T., Hirozane-Kishikawa, T., Dricot, A., Li, N., Berriz, G. F., Gibbons, F. D., Dreze, M., Ayivi-Guedehoussou, N., Klitgord, N., Simon, C., Boxem, M., Milstein, S., Rosenberg, J., Goldberg, D. S., Zhang, L. V., Wong, S. L., Franklin, G., Li, S., Albala, J. S., Lim, J., Fraughton, C., Llamosas, E., Cevik, S., Bex, C., Lamesch, P., Sikorski, R. S., Vandenhaute, J., Zoghbi, H. Y., Smolyar, A., Bosak, S., Sequerra, R., Doucette-Stamm, L., Cusick, M. E., Hill, D. E., Roth, F. P., and Vidal, M. (2005) Towards a proteome-scale map of the human protein-protein interaction network. *Nature* **437,** 1173–1178
22. Clague, M. J., and Urbé, S. (2010) Ubiquitin: same molecule, different degradation pathways. *Cell* **143,** 682–685
23. Clague, M. J., Liu, H., and Urbé, S. (2012) Governance of endocytic trafficking and signaling by reversible ubiquitylation. *Dev. Cell* **23,** 457–467
24. Chung, K. K., Zhang, Y., Lim, K. L., Tanaka, Y., Huang, H., Gao, J., Ross, C. A., Dawson, V. L., and Dawson, T. M. (2001) Parkin ubiquitinates the α-synuclein-interacting protein, synphillin-1: implications for Lewy-body formation in Parkinson disease. *Nat. Med.* **7,** 1144–1150
25. Maekawa, M., Ishizaki, T., Boku, S., Watanabe, N., Fujita, A., Iwamatsu, A., Obinata, T., Ohashi, K., Mizuno, K., and Narumiya, S. (1999) Signaling from Rho to the actin cytoskeleton through protein kinases ROCK and LIM-kinase. *Science* **285,** 895–898
26. Yamauchi, J., Miyamoto, Y., Sanbe, A., and Tanoue, A. (2006) JNK phosphorylation of paxillin, acting through the Rac1 and Cdc42 signaling cascade, mediates neurite extension in N1E-115 cells. *Exp. Cell Res.* **312,** 2954–2961
27. Yamauchi, J., Miyamoto, Y., Murabe, M., Fujiwara, Y., Sanbe, A., Fujita, Y., Murase, S., and Tanoue, A. (2007) Gadd45a, the gene induced by the mood stabilize valproic acid, regulates neurite outgrowth through JNK and the substrate paxillin in N1E-115 neuroblastoma cells. *Exp. Cell Res.* **313,** 1886–1896
28. Yamauchi, J., Miyamoto, Y., Kusakawa, S., Torii, T., Mizutani, R., Sanbe, A., Nakajima, H., Kiyokawa, N., and Tanoue, A. (2008) Neurofibromatosis 2 tumor suppressor, the gene induced by valproic acid, mediates neurite outgrowth through interaction with paxillin. *Exp. Cell Res.* **314,** 2279–2288
29. Yamauchi, J., Torii, T., Kusakawa, S., Sanbe, A., Nakamura, K., Takashima, S., Hamasaki, H., Kawaguchi, S., Miyamoto, Y., and Tanoue, A. (2010) The mood stabilizer valproic acid improves defective neurite formation caused by Charcot-Marie-Tooth disease-associated mutant Rab7 through the JNK signaling pathway. *J. Neurosci. Res.* **88,** 3189–3197
30. Jaworski, J. (2007) ARF6 in the nervous system. *Eur. J. Cell Biol.* **86,** 513–524
31. Burgo, A., Sotirakis, E., Simmler, M. C., Verraes, A., Chamot, C., Simpson, J. C., Lanzetti, L., Proux-Gillardeaux, V., and Galli, T. (2009) Role of Varp, a Rab21 exchange factor and TI-VAMP/VAMP7 partner, in neurite growth. *EMBO Rep.* **10,** 1117–1124
32. Burgo, A., Proux-Gillardeaux, V., Sotirakis, E., Bun, P., Casano, A., Verraes, A., Liem, R. K., Formstecher, E., Coppey-Moisan, M., and Galli, T. (2012) A molecular network for the transport of the TI-VAMP/VAMP7 vesicles from cell center to periphery. *Dev. Cell* **23,** 166–180
33. Wang, J., Morita, Y., Mazelova, J., and Deretic, D. (2012) The Arf GAP ASAP1 provides a platform to regulate Arf4- and Rab11-Rab8-mediated ciliary receptor targeting. *EMBO J.* **31,** 4057–4071
34. Deretic, D., and Wang, J. (2012) Molecular assemblies that control rhodopsin transport to the cilia. *Vision Res.* **75,** 5–10
35. Knödler, A., Feng, S., Zhang, J., Zhang, X., Das, A., Peränen, J., and Guo, W. (2010) Coordination of Rab8 and Rab11 in primary ciliogenesis. *Proc. Natl. Acad. Sci. U.S.A.* **107,** 6346–6351
36. Chiba, S., Amagai, Y., Homma, Y., Fukuda, M., and Mizuno, K. (2013) NDR-mediated Rabin8 phosphorylation is crucial for ciliogenesis by switching binding specificity from phosphatidylserine to Sec15. *EMBO J.* **32,** 874–885
37. Franco, M., Peters, P. J., Boretto, J., van Donselaar, E., Neri, A., D'Souza-Schorey, C., and Chavrier, P. (1999) EFA6, a sec7 domain-containing exchange factor for ARF6, coordinates membrane recycling and actin cytoskeleton organization. *EMBO J.* **18,** 1480–1491
38. Matsuya, S., Sakagami, H., Tohgo, A., Owada, Y., Shin, H. W., Takeshima, H., Nakayama, K., Kokubun, S., and Kondo, H. (2005) Cellular and subcellular localization of EFA6C, a third member of the EFA family, in adult mouse Purkinje cells. *J. Neurochem.* **93,** 674–685
39. Sakagami, H., Suzuki, H., Kamata, A., Owada, Y., Fukunaga, K., Mayanagi, H., and Kondo, H. (2006) Distinct spatiotemporal expression of EFA6D, a guanine nucleotide exchange factor for Arf6, among the EFA6 family in mouse brain. *Brain Res.* **1093,** 1–11
40. Derrien, V., Couillault, C., Franco, M., Martineau, S., Montcourrier, P., Houlgatte, R., and Chavrier, P. (2002) A conserved C-terminal domain of EFA6-family ARF6-guanine nucleotide exchange factors induces lengthening of microvilli-like membrane protrusions. *J. Cell Sci.* **115,** 2867–2879
41. Sakagami, H., Matsuya, S., Nishimura, H., Suzuki, R., and Kondo, H. (2004) Somatodendritic localization of the mRNA for EFA6A, a guanine nucleotide exchange protein for ARF6, in rat hippocampus and its involvement in dendritic formation. *Eur. J. Neurosci.* **19,** 863–870
42. Sironi, C., Teesalu, T., Muggia, A., Fontana, G., Marino, F., Savaresi, S., and Talarico, D. (2009) EFA6A encodes two isoforms with distinct biological activities in neuronal cells. *J. Cell Sci.* **122,** 2108–2118
43. Murphy, J. A., Jensen, O. N., and Walikonis, R. S. (2006) BRAG1, a Sec7 domain-containing protein, is a component of the postsynaptic density of excitatory synapses. *Brain Res.* **1120,** 35–45
44. Scholz, R., Berberich, S., Rathgeber, L., Kolleker, A., Köhr, G., and Kornau, H. C. (2010) AMPA receptor signaling through BRAG2 and Arf6 critical for long-term synaptic depression. *Neuron* **66,** 768–780
45. Morishige, M., Hashimoto, S., Ogawa, E., Toda, Y., Kotani, H., Hirose, M., Wei S., Hashimoto, A., Yamada, A., Yano, H., Mazaki, Y., Kodama, H., Nio, Y., Manabe, T., Wada, H., Kobayashi, H., and Sabe, H. (2008) GEP100 links epidermal growth factor receptor signaling to Arf6 activation to induce breast cancer invasion. *Nat. Cell Biol.* **10,** 85–92
46. Klarlund, J. K., Holik, J., Chawla, A., Park J. G., Buxton, J., and Czech, M. P.

(2001) Signaling complexes of the FERM domain-containing protein GRSP1 bound to ARF exchange factor GRP1. *J. Biol. Chem.* **276,** 40065–40070
47. DiNitto, J. P., Lee, M. T., Malaby, A. W., and Lambright, D. G. (2010) Specificity and membrane partitioning of Grsp1 signaling complexes with Grp1 family Arf exchange factors. *Biochemistry* **49,** 6083–6092
48. Kitano, J., Kimura, K., Yamazaki, Y., Soda, T., Shigemoto, R., Nakajima, Y., and Nakanishi, S. (2002) Tamalin, a PDZ domain-containing protein, links a protein complex formation of group 1 metabotropic glutamate receptors and the guanine nucleotide exchange factor cytohesins. *J. Neurosci.* **22,** 1280–1289
49. Mansour, M., Lee, S. Y., and Pohajdak, B. (2002) The N-terminal coiled coil domain of the cytohesin/ARNO family of guanine nucleotide exchange factors interacts with the scaffolding protein CASP. *J. Biol. Chem.* **277,** 32302–32309
50. Tang, P., Cheng, T. P., Agnello, D., Wu, C. Y., Hissong, B. D., Watford, W. T., Ahn, H. J., Galon, J., Moss, J., Vaughan, M., O'Shea, J. J., and Gadina, M. (2002) Cybr, a cytokine-inducible protein that binds cytohesin-1 and regulates its activity. *Proc. Natl. Acad. Sci. U.S.A.* **99,** 2625–2629
51. Boehm, T., Hofer, S., Winklehner, P., Kellersch, B., Geiger, C., Trockenbacher, A., Neyer, S., Fiegl, H., Ebner, S., Ivarsson, L., Schneider, R., Kremmer, E., Heufler, C., and Kolanus, W. (2003) Attenuation of cell adhesion in lymphocytes is regulated by CYTIP, a protein which mediates signal complex sequestration. *EMBO J.* **22,** 1014–1024
52. Venkateswarlu, K. (2003) Interaction protein for cytohesin exchange factors1 (IPCEF1) bids cytohesin 2 and modifies its activity. *J. Biol. Chem.* **278,** 43460–43469
53. Attar, M. A., Salem, J. C., Pursel, H. S., and Santy, L. C. (2012) CNK and IPCEF1 produce a single protein that is required for HGF-dependent Arf6 activation and migration. *Exp. Cell Res.* **318,** 228–237
54. Ikenouchi, J., and Umeda, M. (2010) FRMD4A regulates epithelial polarity by connecting Arf6 activation with the PAR complex. *Proc. Natl. Acad. Sci. U.S.A.* **107,** 748–753
55. Lim, J., Zhou, M., Veenstra, T. D., and Morrison, D. K. (2010) The CNK1 scaffold binds cytohesins and promotes insulin pathway signaling. *Genes Dev.* **24,** 1496–1506
56. Hofmann, I., Thompson, A., Sanderson, C. M., and Munro, S. (2007) The Arl4 family of small G proteins can recruit the cytohesin Arf6 exchange factors to the plasma membrane. *Curr. Biol.* **17,** 711–716
57. Li, C. C., Chiang, T. C., Wu, T. S., Pacheco-Rodriguez, G., Moss, J., and Lee, F. J. (2007) ARL4D recruits cytohesin-2/ARNO to modulate actin remodeling. *Mol. Biol. Cell* **18,** 4420–4437
58. van den Bosch, M. T., Poole, A. W., and Hers, I. (2014) Cytohesin-2 phosphorylation by PKC relieves the constitutive suppression of platelet dense granule secretion by Arf6. *J. Thromb. Haemost.* **12,** 726–735